[60] Kuhn, R., Rajewsky, K., and Muller, W., Generation and analysis of interleukin-4 deficient mice, *Science* 254, 707-710, 1991.

[61] Renz, C.L. et al., Tryptase levels are not increased during vancomycin-induced anaphylactoid reactions, *Anesthesiology* 89, 620-625, 1998.

[62] Secrist, H., DeKruyff, R.H., and Umetsu, D.T., Interleukin 4 production by CD4+ T cells from allergic individuals is modulated by antigen concentration and antigen-presenting cell type, *J. Exp. Med.* 181, 1081-1089, 1995.

[63] Dorr, R.T., *The Annals of Pharmacotherapy*, Harvey Whitney Books Company, Cincinnati, OH, 1994.

Chapter 13

Reaction-Diffusion Systems: A Mathematical Biology Approach

Miguel A. Herrero

Departamento de Matemática Aplicada, Facultad de Matemáticas, Universidad Complutense de Madrid (Spain)

1-58488-361-8/03/$0.00+$1.50

13.1 Introduction

Reaction-diffusion (RD) systems are mathematical models which provide macroscopic descriptions for the dynamics of media in which random motion and chemical reactions are the major players to be kept track of. In a typical situation, an RD system consists of several coupled differential equations, part of which at least involve space and time dependent variables, and are therefore of the type known as partial differential equations. A particularly simple but important case is provided by single scalar equations, of which the linear diffusion equation is arguably the most relevant example.

Reaction-diffusion systems have been extensively studied during the 20^{th} century. While the mathematical analysis of general, nonlinear RD systems is rather involved, in a number of cases of interest in applications RD equations have been shown to possess a wealth of interesting (and often intriguing) behaviours. These correspond to classes of particular solutions, the study of which often goes under the term of pattern formation theory. These notes are intended to provide an introduction to that subject, which plays an important role in many problems in the natural sciences. However, as it will become apparent from the list of contents, our choice is strongly biased in several aspects. First, the selection of topics made pays particular attention to models in biology and medicine. On the other hand, at the methodological level we have focused on the use of asymptotic methods, which are particularly efficient when the underlying dynamics involves different time and space scales. There is no question about other possible approaches having merits of their own. It seems, however, that the material being reported upon in the sequel is of primary interest for any researcher approaching the field of mathematical biology.

The plan of this chapter is as follows. To start, section 13.2 deals with a general overview of RD systems, followed by a short review of results concerning the linear diffusion equation and its relation to random walks. Then, after quickly remarking on asymptotic states for linear and nonlinear systems, we comment on Turing's classical work on diffusion-driven instability generation in linear systems. After that, the section concludes with a description of a simple (but relevant) model of nonlinear pattern formation, the so-called activator-inhibitor system proposed by Gierer and Meinhardt in 1972.

Section 13.3 deals with particular solutions of RD systems of wave type. As a starting point, we review some classical work on scalar, semi-linear diffusion equations, including the groundbreaking 1937 paper by Kolmogorov, Petrovsky, and Piskunov on the existence of travelling waves for a model arising in biology. We then turn our attention to excitable systems which are of particular interest in life sciences, and recall some relevant cases of wave propagation, including pulses, targets, and spiral waves.

Finally, in section 13.4 we present some selected topics on the mathematical analysis of chemotaxis, that is, on motion of micro-organisms driven by the gradient of an attractant (or repellent) chemical signal. After shortly reviewing the problem of axon growth and neural navigation, we focus on the study of the aggregation properties of a much-studied model, namely the amoeba *Dictyostelium discoideum* (Dd). Phenomena such as chemotactic collapse and stream and spiral motions are considered, always with the help of the asymptotic techniques already introduced in section 13.3.

The material that follows is intended to be suitable for any advanced undergraduate or junior graduate student with some background in differential equations. To keep the flow of the main arguments in the text, lengthy calculations have been omitted, and arguments have been in general condensed. Whenever that occurs, reference is made to those articles or books where additional details can be found.

Last, but not least, I wish to express my sincere thanks to the coordinator of the European Project HPRN-CT-2000-00105, Professor Nicola Bellomo, and to the Director of the Propriano 2001 Summer School on "Using Mathematical Models and Computer Simulation to Improve Cancer Therapy," Professor Luigi Preziosi, for their continuous interest and helpful assistance in all aspects related to the preparation of this work. I am also particularly thankful to Professors Paul Fife and Juan Velázquez for a number of interesting remarks on topics considered in these notes.

13.2 Reaction-Diffusion Systems: Basic Results

In this section we shall recall some relevant facts concerning linear and nonlinear RD systems.

13.2.1 Modelling Assumptions

A reaction-diffusion system of equations is a mathematical formulation of a balance principle. More precisely, let us denote by $u_1, \ldots, u_m$ some quantities depending on space (represented by a vector $\mathbf{x} = (x_1, \ldots, x_n)$, $n \geq 1$) and time (denoted by t). A possible rule for the evolution of the $u_i's$ is provided by

$$\frac{\partial u_i}{\partial t} + \nabla \cdot \mathbf{J}_i = f_i(u_1, \ldots, u_m, \mathbf{x}, t) \,, \qquad 1 \leq i \leq m \,. \tag{13.1}$$

The first term on the left of (13.1) corresponds to local variation of the variable u_i, whereas the second term there accounts for transport of u_i within the surrounding medium. In mathematical terms, the notation $\nabla \cdot \mathbf{J}_i$ means the divergence of the quantity $\mathbf{J}_i$, which is termed as the local flux. A typical choice for $\mathbf{J}_i$ is

$$\mathbf{J}_i = -\mathbf{D}^{(i)}(\mathbf{u}) \nabla u_i + \sum_{k=1}^{m} \mathbf{v}_{ik}(\mathbf{u}) u_k \,, \tag{13.2}$$

where $\mathbf{u} = (u_1, \ldots, u_m)$, and $\mathbf{D}^{(i)}$ is the diagonal matrix $\mathrm{Diag}\{D_1^{(i)}, ..., D_n^{(i)}\}$. The first and second terms in the right of (13.2) are usually referred to as the diffusive and convective components of the flux, respectively: $D_k^{(i)}(\mathbf{u})$ (resp. $\mathbf{v}_{ik}(\mathbf{u})$) are known as the diffusion (resp. convection) coefficients. For instance, assume that $n \geq 1$, $m = 1$ and $\mathbf{D}^{(i)}$, $\mathbf{v}_{ik}$ are constants such that $D_k^{(i)} = D_k > 0$, and $\mathbf{v}_{ik} = \mathbf{v}$ when $i = k$, and $\mathbf{v}_{ik} = 0$ otherwise. Then the transport term in (13.1) is given by

$$\nabla \cdot \mathbf{J} = -\sum_{j=1}^{n} D_j \frac{\partial^2 u}{\partial x_j^2} + \sum_{k=1}^{n} v_j \frac{\partial u}{\partial x_j} .$$

As to the forcing function (13.1), it represents a source (or sink) term, arising for instance from chemical reactions when the u_i denote substances susceptible of recombination. Typical choices for f_i are of a power-like or exponential nature. A simple example, corresponding to the case $n = m = 1$, is provided by $f(u, x, t) = au^k - bu^l$, for some real numbers a, b, k, and l.

13.2.2 Linear Diffusion

A particularly important example of RD systems is the linear diffusion equation, which is obtained by setting in (13.1) $m = 1$, $f = 0$, $v_i = 0$, and $D_i \equiv D > 0$ for $1 \leq i \leq n$. We then obtain

$$\frac{\partial u}{\partial t} = D\Delta u \qquad \text{where} \qquad \Delta u = \sum_{i=1}^{n} \frac{\partial^2 u}{\partial x_i^2} . \tag{13.3}$$

In other words, (13.3) is derived under the assumption that there is no convection in the medium, and the local flux satisfies

$$\mathbf{J} = -D\nabla u ,$$

this last statement being often termed as Fourier's or Fick's law. It is well known that, in order to uniquely determine its solutions, (13.3) has to be supplemented with suitable initial and boundary conditions, thus giving raise to a number of well-posed mathematical problems. One of these is the so-called initial value or Cauchy problem, given by

$$\begin{cases} \dfrac{\partial u}{\partial t} = D\Delta u \qquad \text{when } \mathbf{x} \in \mathbb{R}^n \text{ and } t > 0, \\ \\ u(\mathbf{x}, 0) = u_0(\mathbf{x}) \text{ when } \mathbf{x} \in \mathbb{R}^n , \ t = 0 . \end{cases} \tag{13.4}$$

Here $u_0(x)$ is a given function, on which only mild requirements need to be assumed. One may directly check that a solution of (13.4) is given by

$$u(\mathbf{x}, t) = (4\pi Dt)^{-\frac{n}{2}} \int_{\mathbb{R}^n} e^{-\frac{|\mathbf{x}-\mathbf{y}|^2}{4Dt}} u_0(\mathbf{y})\, d\mathbf{y} , \tag{13.5}$$

where as usual

$$|\mathbf{x} - \mathbf{y}|^2 = \sum_{i=1}^{n} (x_i - y_i)^2 ,$$

provided that the integral above converges in some time interval $0 < t < T \leq \infty$. When

$$|u_0(\mathbf{x})| \leq C\, e^{M|\mathbf{x}|^2} ,$$

for some positive C and M, (13.5) actually yields the only solution to (13.4) (see for instance [30]). A limit case of particular interest appears when $u_0(\mathbf{x})$ reduces to a pointwise discharge of unit intensity (a Dirac delta, or mass, in mathematical terms), $u_0(\mathbf{x}) = \delta(\mathbf{x} - \mathbf{x}_0)$ for some $\mathbf{x}_0 \in \mathbb{R}^n$. This can be considered as an object satisfying $\int_{\mathbb{R}^n} \delta(\mathbf{x} - \mathbf{x}_0)\, d\mathbf{x} = 1$ but such that $\delta(\mathbf{x} - \mathbf{x}_0) = 0$ for any $\mathbf{x} \neq \mathbf{x}_0$. A conceptually more reassuring alternative consists in considering $\delta(\mathbf{x} - \mathbf{x}_0)$ the limit as $j \to \infty$ of a sequence $\{u_{0j}(\mathbf{x})\}$ of smooth and nonnegative functions, each of which vanishes outside the ball $B_j(\mathbf{x}_0) = \{\mathbf{x} : |\mathbf{x} - \mathbf{x}_0| \leq 1/j\}$ and is such that

$$\int_{\mathbb{R}^n} u_{0j}(\mathbf{x})\, d\mathbf{x} = 1 .$$

When such an object is taken as initial value at $t = 0$ in (13.4), (13.5) reduces to

$$\bar{u}(\mathbf{x}, t) = (4\pi Dt)^{-\frac{n}{2}}\, e^{-\frac{|\mathbf{x}-\mathbf{x}_0|^2}{4Dt}} . \tag{13.6}$$

We next remark on two key properties of Equation (13.3), namely its linearity and irreversibility. To begin with, if we consider (13.4) as a black box, which provides a response (output) $u(\mathbf{x}, t)$ whenever a stimulus (input) $u_0(\mathbf{x})$ is fed in, formula (13.5) establishes that response is always proportional to stimulus (multiplying $u_0(\mathbf{x})$ by a factor λ yields $\lambda u(\mathbf{x}, t)$ as a new solution). Furthermore, any finite linear combination of solutions gives again a new solution, and the same happens when infinite such combinations are considered, provided that convergence of the corresponding series can be established. This fact is the basic idea behind Fourier's celebrated separation of variables technique, which is very useful to solve (13.3) in bounded domains with suitable symmetry, and that consists of looking for solutions of the form

$$u(\mathbf{x}, t) = \sum_{j=1}^{\infty} a_j(t) X_j(\mathbf{x}) , \tag{13.7}$$

where the $\{X_j(\mathbf{x})\}$ are a countable family of solutions of a suitable eigenvalue problem, and the $\{a_j(t)\}$ are the corresponding amplitudes which modulate them. Both $\{a_j(t)\}$ and $\{X_j(\mathbf{x})\}$ are to be determined upon substitution of (13.7) into the corresponding boundary value problem for (13.3); see for instance [89] for details.

A second important property of (13.3) is irreversibility, i.e., the fact that changing t by $(-t)$ does not leave (13.3) invariant. Actually, the transformed equation thus

obtained is highly unstable. To wit, consider for instance the initial value problem

$$\begin{cases} \dfrac{\partial u}{\partial t} = -\dfrac{\partial^2 u}{\partial x^2} & \text{when } x \in \mathbb{R},\ t > 0\,, \\ u(x,0) = e^{ikx} & \text{for some } k > 0 \text{ at } t = 0\,. \end{cases} \tag{13.8}$$

A quick check reveals that $u(x,t) = e^{ikx+\Omega t}$ is a solution of (13.8) if

$$\Omega = k^2\,. \tag{13.9}$$

Equation (13.9) is a simple example of a dispersion relation (of which more will be heard in the sequel). It describes the way in which different modes evolve in time (in this case, they are amplified in an exponential way).

A related fact is that solutions to (13.4) do not keep track of most features of their initial values $u_0(x)$. Indeed, (13.5) shows that even if $u_0(x)$ is a highly irregular, discontinuous function, for any positive time t, $u(x,t)$ is infinitely differentiable as a function of x and t. Moreover, if

$$||u_0||_1 = \int_{\mathbb{R}^n} u_0(x)\,dx < \infty\,,$$

it then follows from (13.5) that

$$\max |u(x,t)| \leq Ct^{-\frac{n}{2}}||u_0||_1 \qquad \text{for some } C > 0\,, \tag{13.10}$$

a strong regularising effect. Notice that (13.10) describes both a smoothening and a flattening effect, since the right-hand side of (13.10) decays algebraically to zero as t increases.

13.2.3 Diffusion and Random Walks

The linear diffusion equation (13.3) is a continuum model of a deterministic nature. This means that if we consider, for instance, problem (13.4) and impose some (mild) assumptions on $u_0(x)$, the corresponding solution is uniquely determined for any subsequent times, by means of formula (13.5). Such determinism at a macroscopic scale (i.e., at a continuum level) is however linked to a random character at a microscopic scale (i.e., at a discrete level) which we shortly discuss below.

Consider for simplicity a one-dimensional random walk, i.e., assume that a particle is moving along a line in the form of a series of steps of equal length, each step being taken either in the left or right direction, with equal probability $\frac{1}{2}$. After taking N such steps, the particle could be at any of the points

$$-N, -N+1, \ldots, -1, 0, 1, \ldots, N-1, N\,.$$

The following question naturally arises: what is the probability $W(m,N)$ that the particle arrives at the point m (m being an integer), after suffering N ($N \geq |m|$) displacements?

Suppose for instance that $m > 0$. Then $W(m,N)$ is the probability of taking $(\frac{N+m}{2})$ steps to the right (indeed, $(N+m)$ must be an even number), out of a total of N steps. It then turns out that

$$\begin{aligned} W(m,N) &= (\text{probability corresponding to an arbitrary sequence of paths}) \\ &\quad \times (\text{number of paths leading to place } m) \\ &= \left(\frac{1}{2}\right)^N \binom{N}{\frac{N+m}{2}} = \left(\frac{1}{2}\right)^N \frac{N!}{(\frac{N+m}{2})!(\frac{N-m}{2})!}\,. \end{aligned} \tag{13.11}$$

Formula (13.11) provides an exact answer, but a very cumbersome one (if you doubt this, try counting from one to 9!). However, in some particular (but relevant) cases, one may trade an exact, unwieldy expression by a merely approximate, but convenient, one. This is the rationale behind many so-called asymptotic methods. For instance, assume that

$$N \gg 1 \qquad \text{and} \qquad \frac{m}{N} \ll 1\,, \tag{13.12}$$

these symbols meaning "N is very large" and "m/N is very small," are admittedly not the most precise of the statements (see [4] for a careful definition). We then may take advantage of Stirling's formula

$$N! \sim \frac{\sqrt{2\pi N}\cdot N^N}{e^N} \qquad \text{as} \qquad N \longrightarrow \infty\,,$$

(cf. [4] and [29], Chapter II, Section 10), or more precisely of its logarithmic form

$$log(N!) = \left(N + \frac{1}{2}\right)\log(N) - N + \frac{1}{2}\log(2\pi) + O\left(\frac{1}{N}\right) \qquad \text{as} \qquad N \longrightarrow \infty\,, \tag{13.13}$$

to deduce from (13.11) that

$$W(m,N) \sim \left(\frac{2}{\pi N}\right)^{\frac{1}{2}} e^{-\frac{m^2}{2N}}\,, \tag{13.14}$$

provided that (13.12) holds. Here and henceforth we shall freely use the customary asymptotic notations $\sim$ and $O(\cdot)$. For instance, Equation (13.14) means that, under our current assumptions, the ratio of the quantities appearing at both sides of (13.14) tends to one as $N \longrightarrow \infty$ (although the difference between these two quantities need not become small for large N). On its turn, $O(\frac{1}{N})$ denotes any quantity which in absolute value may be bounded by $\frac{C}{N}$ for some $C > 0$ as $N \longrightarrow \infty$. Here C may be large, but should not depend on N. If we now set

$$x = ml\,, \qquad t = \frac{N}{n}\,,$$

i.e., if we assume that our particle undergoes n displacements by unit time, and introduce a space variable equal to m times the length $l > 0$ of any displacement (no longer assumed to be of unit value), (13.14) yields

$$W(x,t) \sim (4\pi Dt)^{-\frac{1}{2}}\, e^{-\frac{x^2}{4Dt}}\,, \tag{13.15}$$

where

$$D = \frac{nl^2}{2}\,, \tag{13.16}$$

which is a particular case of (13.6) in space dimension $n = 1$. Notice that the mean squared displacement,

$$\langle x^2 \rangle = \int_{-\infty}^{\infty} x^2 W(x,t)\, dx$$

is then such that

$$\langle x^2 \rangle \sim 2Dt\,. \tag{13.17}$$

Relations (13.14) to (13.16) strongly suggest that the continuum equation (13.3) in one space dimension can be considered as a limit model for a one-dimensional random walk when the number of flights N goes to infinity. As a matter of fact, this also happens in higher space dimensions (see for instance [11] for a classical presentation). The random walk just recalled is an example of a stochastic process, a subject for which the reader is referred to [40] and [24] for further information.

13.2.4 General RD Systems: Some Relevant Questions

A type of reaction diffusion system which is often found in applications is the following

$$\begin{cases} \dfrac{\partial u_1}{\partial t} = D_1\, \triangle u_1 + f_1(u_1, \ldots, u_m)\,, \\ \dfrac{\partial u_2}{\partial t} = D_2\, \triangle u_2 + f_2(u_1, \ldots, u_m)\,, \\ \qquad\vdots \qquad\qquad \vdots \\ \dfrac{\partial u_m}{\partial t} = D_m\, \triangle u_m + f_m(u_1, \ldots, u_m)\,, \end{cases} \tag{13.18}$$

where $D_1, D_2, \ldots, D_m$ are given positive constants, and $f_1, \ldots, f_m$ are given (generally nonlinear) functions, whereby coupling between variables $u_1, \ldots, u_m$ is established. Equations (13.18) are said to be of semi-linear type. On setting $\mathbf{f} = (f_1, \ldots, f_m)$, $\mathbf{u} = (u_1, \ldots, u_m)$, and denoting by $\mathbf{D}$ the diagonal matrix with nonzero elements $D_1, \ldots, D_m$, (13.18) is conveniently recast in the form

$$\frac{\partial \mathbf{u}}{\partial t} = \mathbf{D}\triangle \mathbf{u} + \mathbf{f}(\mathbf{u})\,. \tag{13.19}$$

The system obtained by setting $\mathbf{D} = 0$ in (13.19) is usually referred to as the associated kinetic system.

While general enough to account for a wide number of applications, (13.18) is comparatively simple on mathematical terms, since a number of possible features of the process whose modelisation is intended have been ignored. For instance, we have discarded cross-diffusion (which would yield terms such as $\triangle(u_1 + u_2)$ in (13.18)), nonlinear diffusion (corresponding to operators like $\triangle(u_i^r)$ with $r \neq 1$), gradient-dependent forcing terms of the form $f_j(u_1, \frac{\partial u_1}{\partial x_1}, \ldots, \frac{\partial u_1}{\partial x_n}, \ldots, u_m, \ldots)$, and so on. Recalling our discussion in the previous section, we remark that equations of the form (13.18) can be derived as limit dynamics for systems of moderately interacting, randomly moving particles (cf. [69]). The term "moderately" (or short range) refers to suitable assumptions to be made on the way in which the interaction between individual particles is rescaled as the total population increases to infinity. Details can be found in reference [69].

From a mathematical point of view, looking for general solutions of (13.18) is not easy. For one thing, general representation formulae in the spirit of (13.5) are virtually nonexistent (except when the kinetic terms f_i are linear). Moreover, blow-up may occur, i.e., solutions may cease to exist in finite time. This is most simply illustrated by the ordinary differential equation (ODE for short) $u' = u^2$, which has solutions of the form $u_T(t) = (T - t)^{-1}$ for any $T > 0$. A similar phenomenon has been extensively studied in the presence of diffusion, that is, for equations of the type

$$\frac{\partial u}{\partial t} = \triangle u + u^p \qquad \text{with} \qquad p > 1\,.$$

Actually in this equation the interplay between the diffusion and kinetic mechanisms has been shown to provide a countable set of spatio-temporal structures when the blow-up time T (at which solutions become unbounded) is approached. However, out of all these, only that having the simplest space structure (characterised by possessing a single maximum in suitable rescaled variables) is stable; see [37] for a discussion of the one-dimensional case.

In general, the existence of solutions to (13.18) can only be obtained for sufficiently small times. This may be achieved by means of various techniques: fixed point methods [31,55], semigroup theory [72], a priori estimates [21,52], etc. We should also mention that when a higher level of nonlinearity is allowed (for instance, when nonlinear diffusion terms as $\triangle(u^2)$ are considered), classical solutions, that is, functions having all the space and time derivatives required to satisfy the system under consideration at any point, need not exist globally in space, even for arbitrarily short times. As a matter of fact, in that case interfaces may appear at which solutions or their derivatives may develop jumps (see for instance [3] for a review on

an important example). Also, the presence of nonlinear convective terms may lead to shock-wave solutions, which exhibit jumps along some moving shock curves or surfaces (cf. [90]).

However, even if general solution formulae are not available, in many cases one is able to detect particular solutions that often play a key role in the dynamics (i.e., the evolution in space and time of solutions). This is clearly illustrated by the following simple example. Consider the ODE

$$u' = u(1-u). \tag{13.20}$$

Equation (13.20) can be explicitly integrated. However, out of all its infinitely many particular solutions, one of them stands out, namely $\bar{u} = 1$. This is readily seen from the approximate picture of solutions recalled in Figure 13.1 below, that can be obtained from elementary considerations

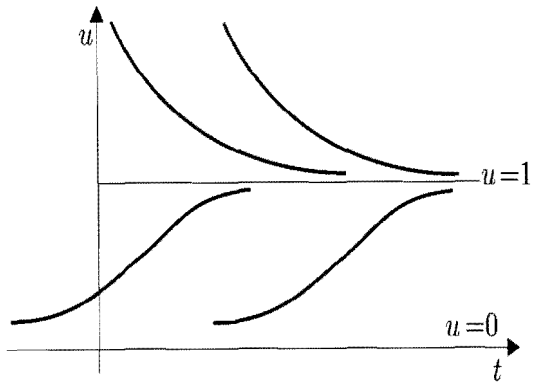

Figure 13.1
The behaviour of solutions of (13.20).

Indeed, $\bar{u} = 1$ is a global attractor for every solution $u \neq 0$ of (13.20). A local (hence weaker) version of this fact, which will be frequently observed in the less trivial examples to follow, is quickly derived by looking for the evolution in time of small perturbations of the explicit solution $\bar{u} = 1$. Namely, let us set

$$u(t) = 1 + z(t) \qquad \text{with} \qquad 0 < |z(0)| \ll 1\,. \tag{13.21}$$

Plugging (13.21) into (13.20), and using the fact that, for small z, $(1+z)^2 \sim 1 + 2z$, we readily see that $z(t)$ satisfies

$$z' = (1+z) - (1+z)^2 \sim 1 + z - 1 - 2z = -z\,.$$

Therefore, at least for small times, $z' \sim -z$, and the subsequent evolution (given approximately by $z(t) = z(0)e^{-t}$) will tend to further damp out the effect of the small perturbation $z(0)$. This is linear stability analysis in a nutshell.

When general systems as (13.18) are considered, a key issue often consists in obtaining relevant particular solutions, that is, solutions displaying asymptotic behaviours that are robust (i.e., do not depend on a particular choice of parameters being made) and at the same time important for the underlying physical or biological problems of which (13.18) is just a model. Consider for instance (13.18) together with initial and boundary conditions for which solutions exist globally in time. In view of our previous remarks, a natural question is the following: what are the possible asymptotics of solutions for large times? Recalling the smoothening feature of linear diffusion illustrated by the regularising effect (13.10), the seemingly obvious answer appears to be that, as time passes, solutions of (13.18) should converge to those of the associated kinetic system, obtained by setting $D_1 = \ldots = D_m = 0$ there.

Indeed, there are many instances in which this is precisely what happens. Consider for instance the case where Ω is a bounded subset of $\mathbb{R}^n (n \geq 1)$ with reasonably smooth boundary, and assume that no-flux conditions are imposed on the boundary of Ω, $\partial\Omega$, viz

$$\frac{\partial u_1}{\partial \mathbf{n}} = \ldots = \frac{\partial u_m}{\partial \mathbf{n}} = 0 \qquad \text{at} \qquad \partial\Omega\,,$$

where $\mathbf{n}$ is the unit normal exterior vector at any point of the boundary $\partial\Omega$. Assume also that our system admits a compact invariant region $\Sigma \subset \mathbb{R}^n$. By this we mean that $0 \in \Sigma$, and if the initial values $\mathbf{u}_0(\mathbf{x}) = (u_{01}(\mathbf{x}), \ldots, u_{0m}(\mathbf{x}))$ lie in the interior of Σ then so does the solution $\mathbf{u} = (u_1, \ldots, u_m)$ for all times $t > 0$. Then it has been shown in [14] that there exits a number $\sigma > 0$, depending on Ω, $\mathbf{f}$, and $D_1, \ldots, D_m$ such that, if

$$\min\{D_1, \ldots, D_m\} > \sigma\,,$$

then $\mathbf{u}$ converges to $\bar{\mathbf{u}}(t)$ as $t \longrightarrow \infty$, where $\bar{\mathbf{u}}(t)$ satisfies

$$\frac{\mathrm{d}\bar{\mathbf{u}}}{\mathrm{d}t} = \mathbf{f}(\bar{\mathbf{u}}) + \mathbf{g}(t)\,, \qquad \bar{\mathbf{u}}(0) = \frac{1}{|\Omega|}\int_\Omega \mathbf{u}_0(x)\,dx\,, \tag{13.22}$$

$|\Omega|$ denotes the volume of Ω, and $|\mathbf{g}(t)| \leq ce^{-\sigma t}$ for some $c > 0$. Then, for sufficiently large times, (13.18) can be replaced by (13.22) under our current assumptions. As a consequence, asymptotically stable equilibria for

$$\frac{\mathrm{d}\mathbf{u}}{\mathrm{d}t} = \mathbf{f}(\mathbf{u})\,,$$

conserve that character for the complete RD system (13.19). As it is well known, the former can be characterised as those points $\tilde{\mathbf{u}}$ such that $\mathbf{f}(\tilde{\mathbf{u}}) = 0$, and for which the eigenvalues λ given by

$$|\nabla \mathbf{f}(\tilde{\mathbf{u}}) - \lambda \mathbf{I}| = 0 ,$$

are such that $\mathrm{Re}\lambda < 0$ (cf. for instance [7] and [12]).

It is now natural to wonder what happens if the assumptions in [14] are not satisfied, something that can be shown to happen if some of the diffusion coefficients in Equation (13.18) are sufficiently small. Then a pattern (that is, an asymptotic state with nontrivial spatial structure) may arise. The simplest candidates for patterns are the stable solutions of the stationary version of (13.18), i.e.,

$$\begin{aligned} D_1 \Delta u_1 + f_1(u_1, \ldots, u_m) &= 0 , \\ &\vdots \\ D_m \Delta u_m + f_m(u_1, \ldots, u_m) &= 0 . \end{aligned} \tag{13.23}$$

However, in many cases, patterns are hard to come by. Consider for instance the semilinear scalar problem

$$\begin{cases} D\Delta u + f(u) = 0 \quad \text{in } \Omega , \\ \dfrac{\partial u}{\partial \mathbf{n}} = 0 \quad \text{in } \partial\Omega . \end{cases} \tag{13.24}$$

Then it has been shown in [56] that, if Ω is convex in $\mathbb{R}^n$, any nonconstant solution of (13.24) is unstable. A similar result has been shown to hold for the system

$$\begin{cases} d_1 \Delta u + f(u, v) = 0 , \\ d_2 \Delta v + g(u, v) = 0 , \end{cases} \tag{13.25}$$

(cf. [48]) provided that

$$\frac{\partial f}{\partial v} \leq 0 , \qquad \frac{\partial g}{\partial u} \leq 0 \quad \text{in } \Omega \quad \text{and} \quad \frac{\partial u}{\partial \mathbf{n}} = \frac{\partial v}{\partial \mathbf{n}} = 0 \quad \text{in } \partial\Omega .$$

However, for any pair $d_1 > 0$, $d_2 > 0$, it is possible to find a domain $\Omega \subset \mathbb{R}^2$ (no longer convex) for which (13.25) possesses a stable, spatially inhomogeneous equilibrium solution [57].

Our previous discussion yields some conditions under which patterns may exist. However, no catalogue of possible patterns has been provided. On the other hand, the question of how a given initial state should evolve into such a pattern has not been addressed. We shall turn our attention to that issue presently.

13.2.5 Linear Theory of Pattern Formation: Turing's Instability

In 1952, A. Turing published a most influential paper [84], in which he argued that reaction-diffusion systems of equations could be actually used as models for

morphogenesis (that is, generation of forms) in living beings. While such approach was not without precedent (see for instance [75]) it certainly gained momentum after Turing's work appeared. The author's vision is concisely described in the abstract of the article:

> "It is suggested that a system of chemical substances, called morphogens, reacting together and diffusing through a tissue, is adequate to account for the main phenomena of morphogenesis. Such a system, although it may originally be quite homogeneous, may later develop a pattern or structure due to an instability of the homogeneous equilibrium, which is triggered off by random disturbances ...",

(cf. [84], p.37). Following [61], we can illustrate this point of view by means of the following simple example. Consider the linear system

$$\begin{cases} \dfrac{\partial u}{\partial t} = \varepsilon \dfrac{\partial^2 u}{\partial x^2} + au - v , \\ \dfrac{\partial v}{\partial t} = \sigma \dfrac{\partial^2 v}{\partial x^2} + u - bv , \end{cases} \tag{13.26}$$

where a and b are some positive parameters, $\varepsilon \geq 0$, and $\sigma \geq 0$. Consider first the kinetic system obtained by setting $\varepsilon = \sigma = 0$ in (13.26). It certainly has a homogenous equilibrium solution $\bar{u} = \bar{v} = 0$. To study its stability properties, we look for perturbations of the form $u_0 e^{\lambda t}$, $v_0 e^{\lambda t}$ with $0 < |u_0| + |v_0| \ll 1$. Plugging these functions into that kinetic system, we see that the exponent λ is such that

$$\lambda = \frac{1}{2}\{(a-b) \pm ((a+b)^2 - 4)^{\frac{1}{2}}\} , \tag{13.27}$$

so that $\bar{u} = \bar{v} = 0$ is asymptotically stable whenever $\mathrm{Re}\lambda < 0$ for both values of λ given in (13.27). It is now easy to draw a stability diagram in terms of the parameters a and b in (13.26) (see Figure 13.2).

Suppose now that we set $\varepsilon = 1$ and $\sigma > 0$, and look for solutions in the form

$$u(x,t) \sim e^{ikx+\lambda t} , \qquad v(x,t) \sim e^{ikx+\lambda t} , \tag{13.28}$$

for some λ and k. This would correspond to solutions which oscillate in space (with period $\frac{2\pi}{k}$) and decrease (or increase) exponentially in time according to the sign of λ. A quick check reveals that λ satisfies an equation similar to Equation (13.27) when one replaces there a by $a(k) = (a - k^2)$ and b by $b(k) = (b + \sigma k^2)$. Therefore, when k is varied, the point $(a(k), b(k))$ moves over the plane (a, b) describing a straight line consisting of points $(\bar{a}, \bar{b})$ having a slope σ, namely $\bar{b} = b + \sigma(a - \bar{a})$. As σ increases, the motion proceeds toward higher values of $\bar{b}$ and smaller values of $\bar{a}$.

Assume now that we start from a value (a, b) located in the stability domain in Figure 13.2. Then, if $\sigma > 0$ is sufficiently large, we may select values $k > 0$ for which $\mathrm{Re}\lambda(k) > 0$ for one of the eigenvalues λ in Equation (13.28). It then turns out that the oscillatory spatial mode with period $\frac{2\pi}{k}$ will grow, and the stationary

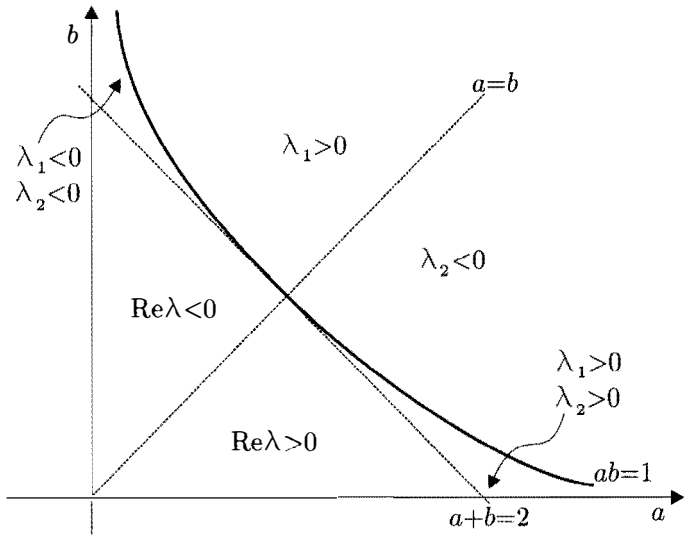

Figure 13.2
The dependence of eigenvalues on coefficients a and b.

state $u = v = 0$ will become unstable with respect to oscillations corresponding to that frequency. Diffusion has therefore destabilised an initially stable homogeneous steady state. This fact is often termed as Turing's instability. The reader is referred to [61], Chapter 5, for a discussion of the various types of instabilities that may arise when systems of type (13.26) are considered in one or two space dimensions.

13.2.6 Nonlinear Pattern Formation: The Activator-Inhibitor Model by Gierer and Meinhardt.

The analysis shortly described in our previous section lies at the heart of the considerable development of the mathematical theory of pattern formation during the last 50 years. Indeed, it is intellectually appealing to think of biological structures (for instance, the limbs of animals) as unfolding out of an almost homogeneous embryo just under the interplay of reaction and diffusion of chemical substances. However, formidable obstacles arise when fitting theory to experiments is attempted (for instance, actual morphogens in animals have proved to be elusive to identification). Even from a merely theoretical point of view, serious difficulties arise at once if linear systems as (13.26) are considered.

Certainly, when it comes to solving equations, linearity is a big bonus. Furthermore, as far as we remain close enough to a given particular solution, any system can be safely approximated by a linear one, namely that obtained by linearising around

such a solution, much as we have done in (13.21). However, such an approximation is no longer valid when perturbations tend to increase, for instance when $\mathrm{Re}\lambda > 0$ in the situation considered in our former section. Once a growing perturbation sets in, there is no way of stopping it in a linear world. To account for actual morphogenesis, one necessarily has to introduce saturation effects, which in mathematical terms amounts to consider nonlinear systems. The price to be paid is that analysis becomes more difficult, a fact that Turing was well aware of. As he explicitly mentions in [84], p. 72, when dealing with nonlinear equations:

> "...The difficulties are, however, such that one cannot hope to have any very embracing theory of such processes, beyond the statement of the equations," although "it may be possible, however, to treat a few particular cases in detail with the aid of a digital computer."

While mathematical analysis and computing have greatly developed since Turing's statement, his remarks continue to provide a sober warning to the limits of quantitative modelling in the life sciences.

However, during the last third of the 20$^{\text{th}}$ Century, analysis of nonlinear models in biology has considerably developed. In this trend, a particularly influential model was the activator-inhibitor system proposed in 1972 by Gierer and Meinhardt (cf. [22]) to account for tentacle formation in hydra. This last is a fresh water polyp whose regenerative properties have attracted much attention over the last two centuries (and that incidentally is also mentioned in [84]).

The main idea in [22] consists in considering a type of pattern formation arising from the interplay of two substances. One of them (called activator), $a(x,t)$, is autocatalytic, and at the same time produces an antagonist (inhibitor), $h(x,t)$. This last counteracts the activator a, but diffuses faster than a does into the surrounding medium. The actual interaction between a and h is prescribed so that:

- a local deviation from an average concentration should increase further (otherwise no pattern would be formed), and
- the increase should not go to infinity, but instead the emerging pattern should reach a stable steady state.

To this end, Gierer and Meinhardt proposed the following system

$$\begin{cases} \dfrac{\partial a}{\partial t} = D_a \dfrac{\partial^2 a}{\partial x^2} + \dfrac{ca^2}{h} - \mu a\,, \\ \dfrac{\partial h}{\partial t} = D_h \dfrac{\partial^2 h}{\partial x^2} + ca^2 - \nu h\,, \end{cases} \tag{13.29}$$

(cf. [22,59]), where c, μ, ν, D_a, and D_h are positive constants. Assume for simplicity that $c = \mu = \nu = 1$. Then $a = h = 1$ is an equilibrium solution of Equation (13.29). If the inhibitor concentration is kept constantly equal to one, then $a = 1$ would be an unstable solution of the first kinetic equation in Equation (13.29), that would reduce to

$$a' = a(a-1)\,.$$

However, if we allow h to change, but we assume that it rapidly achieves its equilibrium to a given activator concentration (which amounts to require $D_h \gg D_a$ in Equation (13.29)), then the kinetic equation for a would be instead

$$a' = \frac{a^2}{a^2} - a = 1 - a\,,$$

for which the corresponding equilibrium $a = 1$ is now a stable one. As stated in [59], "...by a convenient choice of diffusion rates we can achieve local instability with overall stability of the system." It is to be noticed, however, that while numerical simulations in Equation (13.29) are comparatively easy to perform (cf. for instance [59]), the mathematical analysis of (13.29) and related systems (as for instance the model for the unfolding of a planar vascular net proposed in [58]) is yet far from complete in the case of two and three space dimensions; see for instance [78] and [2].

13.3 Wave-Type Solutions

This section is devoted to the study of particular solutions of RD systems. Of these, travelling waves (TW) are specially relevant, since they play a key role in describing propagation phenomena. In a few words, TW are solutions which move at constant velocity without changing shape. We begin by recalling below a classical work which can be rightly considered as the origin of TW theory.

13.3.1 Transition from an Unstable State: The Work by Kolmogorov, Petrovsky, and Piskunov

These authors published their seminal paper [49] in 1937. Motivated by the genetics of natural selection (as described, for instance, in reference [20] quoted therein), they discussed a model to describe the spread of an advantageous gene. In this way they were led to the following problem: to find $v(x,t)$ solution of

$$\frac{\partial v}{\partial t} = k\frac{\partial^2 v}{\partial x^2} + F(v) \qquad \text{when} \quad -\infty < x < \infty\,, \quad t > 0\,, \tag{13.30}$$

$$v(x,0) = H(x)\,, \tag{13.31}$$

where

- F is a continuously differentiable function, such that $F(0) = F(1) = 0$,
- $F(v) > 0$ for $0 < v < 1$, $F'(0) = a > 0$, $F'(v) < a$ for $0 < v < 1$,

(13.32)

- $H(x)$ is a discontinuous step function defined as follows:

(13.33)

$$H(x) = 0 \quad \text{when} \quad x < 0\,, \qquad H(x) = 1 \quad \text{when} \quad x \geq 0\,.$$

The goal of [49] is accurately described by the following excerpts taken from its Introduction:

> "...The domain of densities close to one spreads out, as t increases, from right to left, pushing back the domain of small intensities to the left .... One sees that, as $t \longrightarrow \infty$, the shape of the density curve approaches a limiting shape..." (cf. Figure 13.3 below).

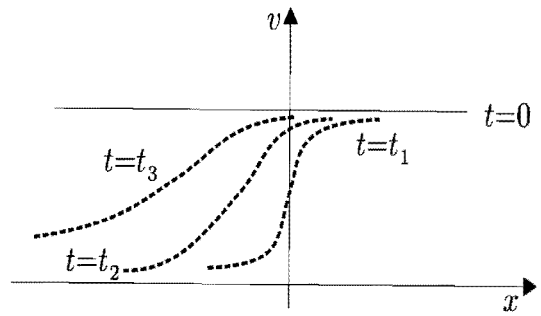

Figure 13.3
The evolution of the density function $v(x,t)$ at times $0 = t < t_1 < t_2 < t_3$

> "...The problem is to find this limit shape of the density curve and the limiting rate of its displacement from right to left. One can show that this last is equal to
>
> $$\lambda_0 = 2\sqrt{ka} \qquad \text{with} \qquad a = F'(0).$$

Note that the kinetic equation associated to (13.30), $v' = F(v)$, has two constant solutions, $v_0 = 0$ and $v_1 = 1$. Of these, the first is unstable, as can be readily

seen from the linearised equation $z' = F'(0)z$. A similar argument shows $v_1 = 1$ to be stable, so that the asymptotics just described above actually correspond to a transition from an unstable state into a stable one.

It is remarkable that the asymptotic speed of propagation of the solution of Equations (13.30) and (13.31) can be computed right away from the knowledge of the diffusion coefficient k and the slope a of function $F(v)$ near $v = 0$. This is rather unusual, as the results in the following sections will show. Incidentally, at this juncture we are taking existence and uniqueness of a solution for granted. This is actually the case, but see the remarks on these issues made at the end of this section.

The approach followed in [49] has become classical, and nowadays is routinely implemented in many problems in applied science. For this reason, some of its main aspects will be briefly sketched here.

To begin with, one looks for solutions of (13.30) of the TW form

$$v(x,t) = v(x+\lambda t) \equiv v(z) \geq 0\,, \tag{13.34}$$

where λ is unknown, and has to be determined in the course of the analysis. Plugging (13.34) into (13.30), we readily see that $v(z)$ should satisfy

$$\lambda \frac{\mathrm{d}v}{\mathrm{d}z} = k\frac{\mathrm{d}^2 v}{\mathrm{d}z^2} + F(v)\,, \qquad -\infty < z < \infty\,. \tag{13.35}$$

Moreover, since we expect v to behave as indicated in Figure 13.3 above, we should also have that

$$\begin{aligned} v(z) &\longrightarrow 0 \quad \text{as} \quad z \longrightarrow -\infty\,, \\ v(z) &\longrightarrow 1 \quad \text{as} \quad z \longrightarrow \infty\,. \end{aligned} \tag{13.36}$$

Together, (13.35) and (13.36) constitute a nonlinear eigenvalue problem, which has to be simultaneously solved for v and λ. It was shown in [49] that this problem has a solution, unique up to translations, whenever $\lambda \geq \lambda_0 = 2\sqrt{ka}$. This was done by rewriting (13.35) as a system

$$\begin{cases} \dfrac{\mathrm{d}v}{\mathrm{d}z} = p\,, \\[2ex] \dfrac{\mathrm{d}p}{\mathrm{d}z} = \dfrac{\lambda p - F(v)}{k}\,. \end{cases} \tag{13.37}$$

Then what is now considered as a standard phase-space analysis was performed. First, one looks for constant solutions of Equation (13.37). These are $(v,p) = (0,0)$ and $(v,p) = (1,0)$. After that, one linearises around them, similarly to what we did for Equation (13.20) in our previous section, to describe the local behaviour of solutions close to these equilibria. When $\lambda \geq 2\sqrt{ka}$, these are as depicted in part *a*) of Figure 13.4. Having done this, the authors undertook a global analysis, eventually showing that there is a trajectory (v,p) connecting both equilibria, see part *b*) in Figure 13.4. Such trajectory corresponds to the sought-for travelling wave, when this last is written in terms of the (v,p) coordinates.

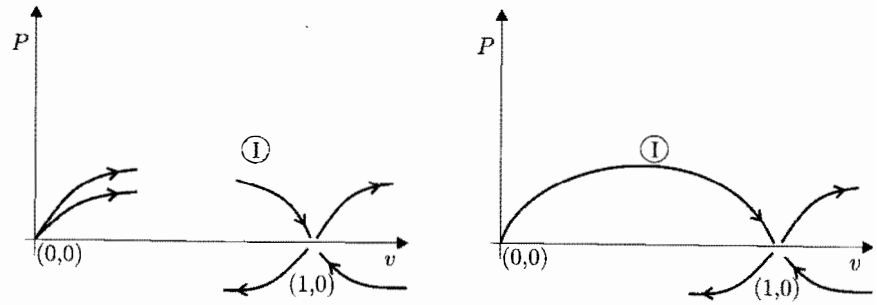

(a) (b)

Figure 13.4

(a) Local portrait of trajectories and equilibria. Point $(0,0)$ is said to be an unstable node, and $(1,0)$ is a saddle point (cf. [7,12] for precise description of these types of equilibria). (b) Global analysis: the trajectory labelled as I corresponds to a TW of (13.30) when $\lambda \geq 2\sqrt{ka}$.

When $\lambda < 2\sqrt{ka}$, trajectories emanating from $(0,0)$ spiral around that point, and cannot therefore provide nonnegative solutions as required in (13.34). The foregoing argument yields the existence of a continuum of TW solutions to (13.30), each of them actually solving the eigenvalue problem (13.35), (13.36) for a value $\lambda \geq \lambda_0$. A key issue in [49] consists of discussing which of these waves is relevant to describe the large-time asymptotics of the problem under consideration. More precisely, the following result is proven in [49] (see also [85]).

There exists a continuously differentiable function $\xi(t)$ such that

$$\xi'(t) \longrightarrow \lambda_0 \equiv 2\sqrt{ka} \quad \text{as} \quad t \longrightarrow \infty\,, \quad \text{and} \tag{13.38}$$

$$v(x - \xi(t), t) \longrightarrow v_0(x) \quad \text{as} \quad t \longrightarrow \infty\,,$$

where v_0 is the solution of Equations (13.35) and (13.36) corresponding to $\lambda \equiv \lambda_0$. Note however that $\xi(t)$ remains undetermined in (13.38). Actually, this "phase indeterminacy," as is often termed, is a property of the model (13.30), and not merely a technical nuisance. For instance, it is known that

$$v(x - 2t, t) \longrightarrow 0 \quad \text{as} \quad t \longrightarrow \infty\,.$$

Furthermore, if $u(x,t)$ is a solution of (13.30) such that $0 < u < 1$ and we assume that $u(x,t)$ converges to some travelling wave as $t \longrightarrow \infty$, and if in addition

$$\lim_{x \to -\infty} e^{\alpha x} u(x,0) = b \neq 0 \quad \text{for some} \quad \alpha \quad \text{with} \quad 0 < \alpha < 1\,,$$

then the velocity of that wave must be $\lambda = (\alpha + \frac{1}{\alpha})\sqrt{ka}$ (cf. [53] for details on these results). Concerning our problem (13.30), (13.31), although it can be said that the x-

profile of $v(x,t)$ approaches that of v_0 (cf. (13.38)), the delicate nature of the results discussed in [53] call attention to possible inaccuracies in any numerical procedure which fail to properly account for the decay of initial values for large $|x|$.

We conclude this section by remarking on the way existence and uniqueness were obtained in [49]. Uniqueness is derived by application of the so-called maximum principle (cf. [21]). Roughly speaking, one assumes the existence of at least two different solutions v_1 and v_2, and considers the equation satisfied by a suitable auxiliary function related to $v_1 - v_2$. Then a contradiction is achieved by examining the sign of the various terms in that equation at the possible local extrema of $v_1 - v_2$.

The existence proof will be briefly sketched below, since it is of a constructive nature, and therefore provides a procedure to approximate the actual solutions. To begin with, let $v_0(x,t)$ be the solution of

$$\begin{cases} \dfrac{\partial v}{\partial t} = k\dfrac{\partial^2 v}{\partial x^2}\,, & -\infty < x < \infty\,, \quad t > 0\,, \\ v(x,0) = H(x)\,. \end{cases} \tag{13.39}$$

Actually, the argument in [49] is carried out for more general initial values than that in Equation (13.39), but consideration of this case is enough for the discussion that follows. A direct check shows that the function

$$\begin{aligned} v_1(x,t) &= v_0(x,t) + \widetilde{v}_1(x,t) \\ &\equiv v_0(x,t) + \frac{1}{2\sqrt{\pi k}} \int_0^t d\eta \int_{-\infty}^{\infty} \frac{e^{-\frac{(x-\xi)^2}{4k(t-\eta)}}}{\sqrt{t-\eta}} F(v_0(\xi,\eta))\, d\xi\,, \end{aligned}$$

is such that $v_1(x,0) = H(x)$ and

$$\frac{\partial v_1}{\partial t} = k\frac{\partial^2 v_1}{\partial x^2} + F(v_0(x,t))\,, \qquad -\infty < x < \infty\,, \quad t > 0\,.$$

A sequence of functions $\{v_i(x,t)\}$ with $i \geq 1$ can be now constructed by means of the rule

$$v_{i+1}(x,t) = v_0(x,t) + \frac{1}{2\sqrt{\pi k}} \int_0^t d\eta \int_{-\infty}^{\infty} \frac{e^{-\frac{(x-\xi)^2}{4k(t-\eta)}}}{\sqrt{t-\eta}} F(v_i(\xi,\eta))\, d\xi\,,$$

and one readily sees that v_{i+1} solves

$$\begin{cases} \dfrac{\partial v_{i+1}}{\partial t} = k\dfrac{\partial^2 v_{i+1}}{\partial x^2} + F(v_i(x,t))\,, & -\infty < x < \infty\,, \quad t > 0\,, \\ v_{i+1}(x,0) = H(x)\,. \end{cases} \tag{13.40}$$

The argument then concludes by showing that $\{v_i(x,t)\}$ converges, as $i \longrightarrow \infty$, towards a continuous function $v(x,t)$, in such a manner that passing to the limit in Equation (13.40) is allowed, so that $v(x,t)$ turns out to solve (13.30) and (13.31).

13.3.2 Bistable Media

In mathematical terms, bistable media are represented by a scalar, semilinear diffusion equation that has two steady states which are stable under sufficiently small perturbations, and an unstable state between them. An important feature of these media is that a sufficiently strong perturbation may induce a transition between the two stable equilibria. The corresponding solutions are called fronts or trigger waves (cf. for instance [17,61]), and will be shortly discussed below. The simplest reaction-diffusion equation of bistable type can be written as follows

$$\frac{\partial u}{\partial t} = D\frac{\partial^2 u}{\partial x^2} + f(u)\,, \qquad -\infty < x < \infty\,, \quad t > 0\,, \tag{13.41}$$

where $D > 0$, and $f(u)$ is a continuously differentiable function as depicted in Figure 13.5 below. Notice that such function $f(u)$ has two stable equilibria at $u = u_1, u_3$, and an unstable one ($u = u_2$), as can be readily seen from the sign of $f'(u)$ at each of these points. A front (or trigger wave) corresponding to the transition from the state u_1 to the state u_3, and moving with velocity c (say, positive) is a function $u(x,t)$ (if any) of the form $u(x,t) = u(x-ct) \equiv u(\xi)$ which solves (13.41), so that

$$Du'' + cu' + f(u) = 0\,, \qquad -\infty < \xi < \infty\,, \tag{13.42}$$

and

$$u(\xi) \longrightarrow u_3 \quad \text{when} \quad \xi \longrightarrow -\infty\,, \qquad u(\xi) \longrightarrow u_1 \quad \text{when} \quad \xi \longrightarrow \infty\,. \tag{13.43}$$

A major difference with the case considered in the previous section is that in general there is no more than one wave speed c for which the eigenvalue problem (13.42) and (13.43) can be solved, uniquely up to translations. Such a solution corresponds to a trajectory in the phase space associated to (13.42) joining the two saddle points $(u_1, 0)$ and $(u_3, 0)$. In most cases, the actual value of c can only be computed numerically, again in sharp contrast with the KPP model discussed before. An important exception is provided by the following example

$$\frac{\partial u}{\partial t} = \frac{\partial^2 u}{\partial x^2} + u(1-u)(u-a) \qquad \text{with} \qquad 0 < a < 1\,. \tag{13.44}$$

In this case, the function

$$v(\xi) = \left(1 + e^{\frac{\xi}{\sqrt{2}}}\right)^{-1}\,, \qquad \xi = x - ct\,, \tag{13.45}$$

is a travelling wave with speed

$$c = \sqrt{2}\left(\frac{1}{2} - a\right)\,. \tag{13.46}$$

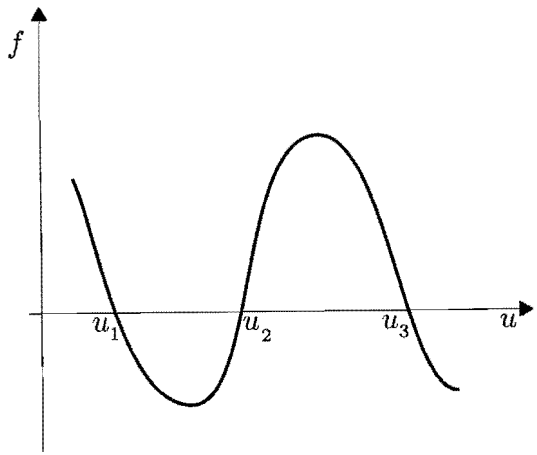

Figure 13.5
A function $f(u)$ characterising a bistable medium.

Notice that the sign of c coincides with that of $(\frac{1}{2} - a)$. Actually, in the general case (13.42) that sign is a feature of the wave motion that can be easily determined from the very beginning. Indeed, on assuming further that $u'(\xi) \longrightarrow 0$ as $\xi \longrightarrow \pm\infty$ (a fact that can be checked a posteriori, and that (13.45) certainly satisfies), we may multiply both sides of (13.42) by $u'(\xi)$ and then integrate from $-\infty$ to ∞ to eventually obtain

$$c = \left(\int_{u_1}^{u_3} f(s)ds\right)\left(\int_{-\infty}^{\infty} (u'(s))^2\, ds\right)^{-1}, \qquad (13.47)$$

so that $\mathrm{sgn}(c) = \mathrm{sgn}\int_{u_1}^{u_3} f(s)\, ds$, and fronts move either way (or remain stationary) according to the actual shape of $f(u)$ in Figure 13.5.

In the general case, besides proving the existence of travelling waves for Equation (13.41), the question naturally arises of ascertaining to what extent such waves, whenever they exist, are relevant for the dynamics of the corresponding equations. More precisely, we may wonder whether fronts are stable, or if they are the only possible propagation patterns in such media, what happens when two such waves collide, and so on. Also, we may be interested in discussing wave propagation for these types of equations in higher space dimensions. This last question will be addressed later on (cf. section 13.3.4). Here we shall briefly consider the question of stability.

Consider again Equation (13.41), and let $\Phi(x - ct) \equiv \Phi(\xi)$ be a travelling wave of that equation, so that $\Phi(\xi)$ solves (13.42). Then, on setting $w = \Phi'(\xi)$, w in turn satisfies

$$A(w) \equiv Dw'' + cw' + f'(\Phi)w = 0\,. \qquad (13.48)$$

Suppose now that we consider solutions initially close to the wave Φ, i.e., such that

$$u(x,t) = \Phi(\xi) + z(\xi,t) \quad \text{with} \quad 0 < |z| \ll \Phi\,,$$

at some initial time. Then, on expanding

$$f(\Phi + z) = f(\Phi) + f'(\Phi)z + \dots\,,$$

we see that to the lowest order, the perturbed function $z(\xi,t)$ should satisfy

$$\frac{\partial z}{\partial t} = A(z)\,,$$

with $A(z)$ as in (13.48). Since this operator has a zero eigenvalue, waves are determined up to translations (as it has already been mentioned), and a natural definition of stability would be this:

$\Phi(\xi)$ is stable if, whenever $z(\xi,t)$ is initially small,

$$(\Phi(\xi) + z(\xi,t)) \longrightarrow \Phi(\xi + h) \text{ as } t \longrightarrow \infty, \text{ for some finite constant } h.$$

The stability of fronts solving Equations (13.42) and (13.43) was established by Fife and McLeod in two influential papers (cf. [18,19]). Consider for instance the case when $f(u)$ is as in Figure 13.5 with $u_1 = 0$ and $u_3 = 1$. It is then known that such an equation has a unique (up to translations) monotone travelling front of the form $U(x-ct)$ (see for instance [44]). Suppose now that a continuous function $\varphi(x)$ is given, such that $0 \le \varphi(x) \le 1$, and

$$\lim_{x\longrightarrow\infty} \varphi(x) > u_2\,, \qquad \lim_{x\longrightarrow-\infty} \varphi(x) < u_2\,.$$

Then a result in [18] ensures that there exists a finite value x_0 such that the solution of (13.41) over the whole line with initial value $\varphi(x)$ approaches toward $U(x - ct - x_0)$ exponentially in time, and uniformly on x.

There are situations in which the solution of the initial value problem (13.41) will develop into a pair of fronts moving in opposite directions. For instance, let $f(u)$ be as before, and suppose also that $\int_0^1 f(s)\, ds > 0$. Assume now that $\varphi(x)$ is a continuous function such that $0 \le \varphi(x) \le 1$ and

$$\lim_{|x|\longrightarrow\infty} \varphi(x) < u_2\,, \qquad \phi(x) > u_2 + \eta \quad \text{for} \quad |x| < L\,,$$

where η and L are some positive numbers. Then, as proven in [18], if L is sufficiently large (depending on η and f), there exist constants x_0, x_1, K, and ω (the last two positive) such that the solution $u(x,t)$ of (13.41) with initial value $\varphi(x)$ satisfies

$$\begin{aligned} |u(x,t) - U(x - ct - x_0)| &< Ke^{-\omega t} \quad \text{when} \quad x < 0\,, \\ |u(x,t) - U(-x - ct - x_1)| &< Ke^{-\omega t} \quad \text{when} \quad x > 0\,, \end{aligned}$$

where $U(x - ct)$ is as in our previous case.

Front waves are known to be the only possible nontrivial patterns of (13.41) (cf. [17,61]). From a biological point of view, bistable media are far from satisfactory for many modelling purposes. In particular, a wave propagating in such medium will leave any point forever excited after reaching it. We shall next see which modifications are to be introduced in this model to dispense with this unwanted feature.

13.3.3 Excitable Systems: Pulses

In rather informal terms, an excitable system can be described by:

- having one stable equilibrium, so that any small enough perturbation around it rapidly decays towards that point, and
- possessing such kinetic terms so as to ensure that any sufficiently large perturbation around the stable equilibrium undergoes a prolonged excursion before eventually returning to it.

In a simple case, an excitable system can be obtained from two coupled equations, corresponding respectively to a bistable medium and a restoring mechanism. As we shall presently see, besides fronts, such systems admit a different type of travelling waves named pulses. These are characterised by the fact that they approach toward the same resting state, both ahead and behind the moving perturbation.

One of the most relevant examples of excitable systems is provided by the FitzHugh-Nagumo (FHN) equations. These were derived as a model simpler than, but qualitatively similar to, the celebrated Hodgkin-Huxley equations for excitation and conduction in nerve (cf. [39] and also [15]). A particular example of the (FHN) equations is the following

$$\frac{\partial v}{\partial t} = \frac{\partial^2 v}{\partial x^2} + z + f(v), \text{ with } f(v) = v(1-v)(v-a) \text{ and } 0 < a < 1 \quad (13.49)$$

$$\frac{\partial z}{\partial t} = \varepsilon v\,, \qquad \text{with} \quad \varepsilon > 0\,. \quad (13.50)$$

In the sequel we shall closely follow the arguments in [10], and look for solutions of Equations (13.49) and (13.50) of the form

$$v(x,t) = v(x+\theta t)\,, \qquad z(x,t) = z(x+\theta t) \qquad \text{for some} \quad \theta > 0\,. \quad (13.51)$$

On setting $\xi = x + \theta t$, we readily see that such solutions should satisfy

$$\frac{\mathrm{d}^2 v}{\mathrm{d}\xi^2} - \theta\frac{\mathrm{d}v}{\mathrm{d}\xi} + f(v) - z = 0\,, \quad (13.52)$$

$$\theta\frac{\mathrm{d}z}{\mathrm{d}\xi} = \varepsilon v\,. \quad (13.53)$$

Equations (13.52) and (13.53) can be transformed into a system of three autonomous, first-order differential equations by writing $\frac{\mathrm{d}v}{\mathrm{d}\xi} = h$. Hence, the corresponding phase space of variables (v, h, z) is also three-dimensional and its phase portrait (i.e., the plotting of its trajectories) is more involved than the two-dimensional cases considered in our previous sections. However, the analysis of (13.52) and (13.53) greatly simplifies if we assume

$$0 < \varepsilon \ll 1\,. \quad (13.54)$$

Indeed, introducing a small parameter allows us to make use of singular perturbation techniques, a most powerful tool in analysis (see for instance [4] for a detailed account). From now on, we assume that (13.54) holds, and proceed to describe how a first approximation to a pulse of (13.49), (13.50) can be obtained. What we want is to obtain a solution of the form (13.51), such that the v-component behaves as indicated in the Figure 13.6.

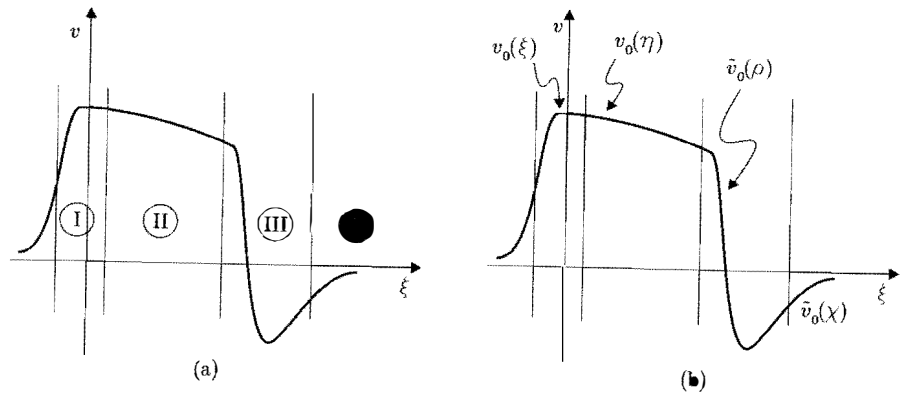

Figure 13.6

(a) The v-component of a pulse solution of (13.49), (13.50). Various relevant regions in the graph of v are denoted as I, II, III, and IV. (b) The detailed structure of the pulse as described in the text.

We now make precise some assumptions on the form of the sought-for pulse. To begin with, we assume $\theta > 0$ to be of order one, and expect $z(\xi)$ to decay to zero as $\xi \longrightarrow -\infty$. Setting $\varepsilon = 0$, we may discard the right-hand side in (13.53) to obtain

$$\frac{\mathrm{d}z}{\mathrm{d}\xi} = 0\,, \qquad z(\xi) \longrightarrow 0 \quad \text{as} \quad \xi \longrightarrow -\infty\,.$$

This gives at once $z(\xi) = 0$, which upon substitution in (13.49) yields

$$\frac{\partial v}{\partial t} = \frac{\partial^2 v}{\partial x^2} + v(1-v)(v-a)\,.$$

Solving this equation with the condition $v(\xi) \longrightarrow 0$ as $\xi \longrightarrow -\infty$, we obtain the analogue of (13.45), viz.

$$v_0 = \left(1 + e^{-\frac{\xi}{\sqrt{2}}}\right)^{-1}, \qquad \theta = \theta_0 = \sqrt{2}\left(\frac{1}{2} - a\right), \tag{13.55}$$

which accounts for the profile of v in Region I in Figure 13.6a. Note that $v_0(\xi) \longrightarrow 1$ as $\xi \longrightarrow \infty$, so that $v_0(\xi)$ actually represents a front instead of a pulse. However, $v_0(\xi)$ is easily seen not to provide a uniformly valid approximation for large values of ξ. Indeed, from (13.53) we see that the exact expression for $z(\xi)$ is

$$z(\xi) = \frac{\varepsilon}{\theta}\int_{-\infty}^{\xi} v(r)\,dr\,.$$

Upon replacing $v(r)$ by $v_0(r)$ there, we readily check that z becomes of order one (and therefore cannot be neglected in (13.53)) at distances $\xi = O(\frac{1}{\varepsilon})$. This suggests introducing new variables to analyse Region II in Figure 13.6a as follows

$$\eta = \varepsilon\xi\,,\ u(\eta,\varepsilon) = v(\xi,\varepsilon)\,,\ y(\eta,\varepsilon) = z(\xi,\varepsilon)\,. \tag{13.56}$$

Equations (13.52) and (13.53) then transform into

$$\varepsilon^2\frac{\mathrm{d}^2u}{\mathrm{d}\eta^2} - \varepsilon\theta\frac{\mathrm{d}u}{\mathrm{d}\eta} + f(u) - y = 0\,, \tag{13.57}$$

$$\theta\frac{\mathrm{d}y}{\mathrm{d}\eta} = u\,. \tag{13.58}$$

On setting above $\theta = \theta_0$ (cf. (13.55)) and $\varepsilon = 0$, we obtain

$$f(u_0) = y_0\,, \tag{13.59}$$

which upon substitution in (13.58) gives $\mathrm{d}\eta = \theta_0\left[\frac{f'(u_0)}{u_0}\right]\mathrm{d}u_0$, whence

$$\eta = \theta_0\left[-\frac{3}{2}u_0^2 + 2(1+a)u_0 - a\log|u_0| + C\right], \tag{13.60}$$

besides the trivial solution $u_0 = 0$. Notice that (13.60) defines u_0 as a multivalued function of η. Let us write $u_{\min}$ (resp. $u_{\max}$) to denote the point where $f(u)$ achieves its minimum (resp. its maximum) in $[0, 1]$, and let us select $u_0(\eta)$ as the solution of (13.60) in the branch where $u_0 \geq u_{\max}$. This function will describe (to the lowest order) our pulse in terms of v in Region II (cf. Figure 13.6). To allow for matching with Region I, we also require

$$\lim_{\eta\longrightarrow 0} u_0(\eta) = v_0(\infty) = 1\,, \qquad y_0(0) = 0\,.$$

From (13.60) we deduce that $u_0(\eta)$ decreases as η increases, but is bounded from below by a positive constant in the branch under consideration. Therefore,

patching together $v_0(\xi)$ and $u_0(\eta)$ still does not provide a uniformly valid representation for the pulse. To this end, we need to introduce a further layer, where a downjump will occur. Suppose that this will happen near a value $\eta = \eta_d$, at which z will achieve a (unknown as yet) value $K_0 > 0$. We then introduce new variables given by

$$\varepsilon\rho = \eta - \eta_d\,, \qquad \tilde{v}_0(\rho,\varepsilon) = u_0(\eta,\varepsilon)\,.$$

Then, on setting $\frac{d\tilde{v}_0}{d\rho} = \tilde{w}_0$, we arrive at

$$\frac{d\tilde{w}_0}{d\rho} = \theta_0\tilde{w}_0 - f(\tilde{v}_0) + K_0\,, \tag{13.61}$$

together with boundary conditions

$$\begin{aligned}\tilde{v}_0(\rho) &\longrightarrow \tilde{\mathrm{U}} \quad \text{as} \quad \rho \longrightarrow -\infty\,,\\ \tilde{v}_0(\rho) &\longrightarrow \tilde{\mathrm{V}} \quad \text{as} \quad \rho \longrightarrow \infty\,,\end{aligned} \tag{13.62}$$

where $\tilde{\mathrm{U}} = u_0(\eta_d)$ and $\tilde{\mathrm{V}}$ are not determined yet. Note that the speed of the downjump has been already fixed, and is equal to θ_0, the corresponding value at the upjump. It is a most remarkable fact that, as shown in [10], this nonlinear eigenvalue problem has a unique solution only for a particular value of K_0. More precisely, in terms of $\tilde{v}_0$, this solution is

$$\tilde{v}_0(\rho) = \frac{\tilde{\mathrm{U}}e^{-h\rho} + \tilde{\mathrm{V}}}{1 + e^{-h\rho}}\,, \tag{13.63}$$

where

$$\sqrt{2}h = \tilde{\mathrm{U}} - \tilde{\mathrm{V}}\,,\quad \tilde{\mathrm{U}} = \tfrac{2+2a}{3}\,,\quad \tilde{\mathrm{V}} = \tfrac{2a-1}{3}\,,\quad \text{and}\quad K_0 = -2f_{\inf}\,,$$

with $f_{\inf} \equiv$ value of f at its inflection point, that is (13.64)

$$f_{\inf} = \tfrac{1}{27}(1+a)(2-a)(2a-1)\,.$$

Incidentally, this result is obtained by looking for solutions of Equations (13.61) and (13.62) such that $\tilde{w}(\tilde{v})$ is a polynomial: $\tilde{w}(\tilde{v}) = \lambda(\tilde{v} - \mathrm{V})(\mathrm{U} - \tilde{v})$ for some λ, where V, U are the extreme roots of $f(v) + K = 0$. Since $\theta_0 > 0$, $0 < a < \frac{1}{2}$, and $K_0 > 0$, by (13.64), $\tilde{\mathrm{V}} < 0$, and to complete the picture a further piece is needed, namely an outer solution which increases from $v = \tilde{\mathrm{V}}$ at $\eta = \eta_d$ to $v = 0$ as $\eta \longrightarrow \infty$. This solution is provided by $\tilde{u}_0$, where this time the branch where $u < 0$ has to be selected. To deal with the corresponding region, it is also convenient to introduce a new variable by setting $\chi = \varepsilon\rho$. In this way the leading approximation to the v-component of the pulse has been sketched. Higher-order approximations (involving powers of ε in the corrective terms derived) can then be obtained by perturbative analysis, as is done in [10].

Concerning the procedure thus sketched, some remarks are in order. First, Equation (13.57) can be shown to admit also solutions for which

$$\theta = \mathrm{O}(\sqrt{\varepsilon}) \,, \tag{13.65}$$

(see [10], Section 4). Therefore, for given values of a and ε, two pulse solutions are possible: a fast one (with $\theta = \mathrm{O}(1)$) and a slow one (satisfying (13.65)). As the authors of [10] observed, "... it is believed that the larger value of θ corresponds to a stable solution, and the smaller value to an unstable one." As a matter of fact, the stability of fast pulses was later proven in [43]. A second important remark is that pulses are not the only new kind of patterns arising in (13.49), (13.50). For instance, periodic wavetrains can be constructed by methods closely related with those described above. We shall not pursue this matter any further here, and refer instead to [10] and [25] for details.

Let us summarise a bit. We have just recalled how pulses can be constructed for the FHN model (13.49), (13.50) under two key hypotheses: the precise form of $f(u)$ in (13.49) and the small parameter assumption (13.54). This last can be dispensed with (i.e., ε can be takcn to be of order one) if, instead of selecting $f(u)$ as in (13.49), we make the explicit choice

$$f(u) = H(u-a) - u \qquad \text{with} \qquad 0 \leq a \leq \frac{1}{2} \,,$$

where $H(s)$ is the step function defined in (13.33). The corresponding study can be found in [76].

To conclude this section, we point out that we have merely scratched at the surface of a large body of results available for pulse propagation in excitable systems. We just refer here to [77] and [45] for further glimpses at the corresponding theory.

13.3.4 Excitable Systems: Targets and Spirals

In our previous sections we have been concerned with waves propagating in one-dimensional media. We shall consider now some particularly relevant structures appearing in higher-dimensional situations. For instance, rotating spirals and concentric circular waves (called targets) are observed in various chemical and biological settings (see for instance [61,63]). We shall define below in a precise manner such types of solutions, describe some reaction-diffusion systems where they appear, and remark on the relevance of these systems from a modelling point of view.

Let us discuss spiral waves first. To this end, consider the following system in two space dimensions

$$\begin{cases} \dfrac{\partial u}{\partial t} = D\triangle u + \lambda(A)u - \omega(A)v \,, \\ \dfrac{\partial v}{\partial t} = D\triangle v + \omega(A)u + \lambda(A)v \,, \end{cases} \tag{13.66}$$

where $D > 0$, and λ, ω are given functions of $A = (u^2 + v^2)^{\frac{1}{2}}$. The system of equation (13.66) is generally referred to as a $\lambda - \omega$ system. A key assumption to be made in (13.66) is the following:

for some $a > 0$, $\lambda(A)$ is a continuous, decreasing, and positive function in an interval $[0, a)$, and $\lambda(a) = 0$. (13.67)

Condition (13.67) ensures that the kinetic system associated to (13.66) has a stable limit cycle, which corresponds in phase space to a monoparametric family of periodic solutions differing from each other only in a phase shift. Such a limit cycle has amplitude a and frequency $\omega(a)$. It is often convenient to rewrite (13.66) in a more compact manner by setting

$$\mathrm{w} = u + iv \,, \tag{13.68}$$

in which case (13.66) reduces to

$$\frac{\partial \mathrm{w}}{\partial t} = (\lambda + i\omega)\mathrm{w} + D\triangle \mathrm{w} \,. \tag{13.69}$$

It is then natural to look for solutions of the form

$$\mathrm{w} = Ae^{i\phi} \,, \tag{13.70}$$

where A is an amplitude variable, and ϕ is the corresponding phase. Plugging (13.70) into (13.69), one readily sees that A and ϕ should satisfy

$$\begin{cases} \dfrac{\partial A}{\partial t} = A\lambda(A) - DA|\nabla\phi|^2 + D\triangle A \,, \\ \dfrac{\partial \phi}{\partial t} = \omega(A) + \dfrac{2D}{A}(\nabla A \cdot \nabla\phi) + D\triangle\phi \,. \end{cases} \tag{13.71}$$

An m-armed spiral wave of (13.69) is defined as a solution of the form (13.70), where

$$A = A(r) \,, \qquad \phi = \Omega t + m\theta + \psi(r) \,, \tag{13.72}$$

and (r, θ) denote polar coordinates in $\mathbb{R}^2$, $A(r)$, $\psi(r)$ (respectively Ω) are functions (resp. a constant) to be determined, and $m \geq 1$ is a positive integer.

In view of (13.71), the corresponding equations for amplitude and phase read then

$$\begin{cases} D(A'' + \frac{A'}{r}) + A\left(\lambda(A) - D(\psi')^2 - \frac{Dm^2}{r^2}\right) = 0 \,, \\ D\left(\psi'' + (\frac{1}{r} + \frac{2A'}{A})\psi'\right) = \Omega - \omega(A) \,. \end{cases} \tag{13.73}$$

System (13.73) has to be supplemented with suitable boundary conditions

$$A(0) = \psi'(0) = 0\,, \qquad A(r) \longrightarrow A(\infty) \quad \text{as} \quad r \longrightarrow \infty\,. \tag{13.74}$$

Notice that from this and (13.73) one readily sees that

$$\psi'(\infty) = \left(\frac{\lambda(A_\infty)}{D}\right)^{\frac{1}{2}}\,, \qquad \Omega = \omega(A_\infty)\,, \tag{13.75}$$

which in particular shows that the amplitude at infinity determines the frequency Ω. From now on, we shall set $D = 1$ for simplicity. It has been shown in [13] that, when $m = 1$, there exists a solution of (13.73), (13.74) provided that in addition to (13.67) the following hypothesis is made:

$\omega = \omega(A)$ is continuous in $[0, a]$, and there exist $\varepsilon \geq 0$ and $\mu > 0$ such that

$$|\omega(a) - \omega(A)| \leq \varepsilon(a - A)^{1+\mu} \quad \text{when} \quad 0 \leq A \leq a\,. \tag{13.76}$$

More precisely, the existence proof provided in [13] (which consists in a topological fixed point argument) yields the existence of a logarithmic spiral wave, i.e., a function $w = u + iv$ such that

$$\begin{cases} u \equiv A(\infty)\cos\Omega t + \theta + c\log r\,, \\ v \equiv A(\infty)\sin\Omega t + \theta + c\log r\,, \end{cases} \tag{13.77}$$

where

$$c = \frac{1}{a^2}\int_0^\infty sA^2(s)(\omega(A) - \omega(A(s)))\,ds\,.$$

Before a discussion on extensions and improvements of this early result, we remark on the structure requirements made in (13.66) and (13.67). In this respect, it should be noticed that a large class of RD systems can be approximated, in some asymptotic limit, by means of $\lambda - \omega$ equations (cf. for instance [13] and [27]). More precisely, let us follow [27] and consider the system

$$\begin{cases} \dfrac{\partial A_1}{\partial t} = F_1(\mu, A_1, A_2) + \nabla\cdot(D_1(\mu, A_1, A_2)\nabla A_1)\,, \\ \dfrac{\partial A_2}{\partial t} = F_2(\mu, A_1, A_2) + \nabla\cdot(D_2(\mu, A_1, A_2)\nabla A_2)\,, \end{cases} \tag{13.78}$$

where μ represents some nondimensional parameter, and suppose that at some critical value $\mu = \mu_0$ the diffusionless (kinetic) equations, obtained by setting $D_1 = D_2 = 0$ above, are such that a bifurcation from a stable state (A_1^0, A_2^0) to a stable limit cycle occurs (in mathematical terms this is called a Hopf bifurcation). Then, arguing as in [27], Appendix A, we assume $0 < \mu - \mu_0 \ll 1$, and look for solutions of the form

$$A_i \sim A_i^0 + (\mu - \mu_0)^{\frac{1}{2}}A(T, \tilde{\mathbf{x}})a_i\cos\left(\omega t + \gamma_i + \phi(T, \tilde{\mathbf{x}})\right)\,, \quad i = 1, 2$$

where $\tilde{\mathbf{x}} = (\tilde{x}_1, \tilde{x}_2) = (\mu - \mu_0)^{\frac{1}{2}}(x_1, x_2)$, a_i and γ_i are suitable constants, and $T = (\mu - \mu_0)t$. Then the overall amplitude and phase $A = (A_1^2 + A_2^2)^{\frac{1}{2}}$ and ϕ are shown to evolve according to the equations

$$\begin{pmatrix} \dfrac{\partial A}{\partial T} \\ A\dfrac{\partial \phi}{\partial T} \end{pmatrix} = \begin{pmatrix} \cos z & -\sin z \\ \sin z & \cos z \end{pmatrix}\begin{pmatrix} \Delta A - A|\nabla\phi|^2 \\ A\Delta\phi + 2\nabla A\cdot\nabla\phi \end{pmatrix} + \begin{pmatrix} A(1 - A^2) \\ qA^3 \end{pmatrix}\,, \tag{13.79}$$

where q and z are certain constants determined from the original system (13.78). In particular, when $D_1 = D_2$, then $z = 0$, and the following $\lambda - \omega$ system is obtained

$$\begin{cases} \dfrac{\partial A}{\partial T} = \Delta A - A|\nabla\phi|^2 + A(1 - A^2)\,, \\ A\dfrac{\partial \phi}{\partial T} = A\Delta\phi + 2\nabla A\cdot\nabla\phi + qA^3\,. \end{cases} \tag{13.80}$$

However, since $\omega(A) = qA^2$ in (13.80), condition (13.76) is not fulfilled, and further analysis is required to ensure the existence of spiral waves in this case. In [27], a variety of arguments (analytical and numerical) have been presented to obtain the existence of Archimedean spiral waves of (13.80) (these satisfy $\psi(r) \sim kr$ as $r \longrightarrow \infty$ in (13.72)) for all values of q. More precisely, existence is proven for $q = 0$, which is the startpoint to deal with the case $0 < |q| \ll 1$ via perturbation theory. Spiral waves are also obtained for $|q| \gg 1$, and then a numerical continuation argument is produced to derive the existence of spiral waves for intermediate values of q. The question of the stability of spirals is also addressed, and the author concludes that when $q = 0$, one-armed spirals are stable, while multi-armed ones are not. It is also remarked therein that perturbative arguments strongly suggest that one-armed spirals continue to be stable for small values of $|q|$.

The results just recalled above belong to what could be called early spiral wave theory for excitable systems. This last has greatly developed ever since, and a wealth of analytical and numerical results are now available for a number of model RD systems. We refer to [25,46,61,63,91,92] for further material on that topic.

Before shifting arguments, a further remark is in order. If we change variables in (13.79) by setting $W = Ae^{i\phi}$ (cf. (13.70)), we obtain the so-called Ginzburg-Landau (GL) equation

$$\frac{\partial W}{\partial T} = \alpha W - \beta|W|^2W + d\Delta W\,, \tag{13.81}$$

where α, β, and d are some complex coefficients that can be determined from the original system (13.78). This is a particular example of the so-called amplitude equations, that have been extensively used in the physical literature to describe pattern formation resulting from a Hopf's bifurcation in an underlying kinetic system. We

shall not pursue this matter any further here, but refer instead to [51] and [16] for additional information.

We next turn our attention to target patterns. These may be thought of as a travelling wave train of concentric circles propagating from a centre, which is often referred to as a pacemaker. We shall describe below a way of characterising target patterns in RD systems, and from that we will derive some information about media where such a type of wave propagation is sustained.

Specifically, following [26] we consider a system given in vector form by

$$\frac{\partial \mathbf{A}}{\partial t} = \mathbf{F}(\mathbf{A}) + \varepsilon D \triangle \mathbf{A} + \varepsilon \mathbf{g}(\mathbf{x}, \mathbf{A}) , \tag{13.82}$$

where $\mathbf{A} = (A_1, A_2)$, $D > 0$, $0 < \varepsilon \ll 1$, and $\mathbf{g}(\mathbf{x}, \mathbf{A})$ is a bounded function of its arguments. On the kinetic term $\mathbf{F}(\mathbf{A})$ we assume conditions so as to ensure that the autonomous system

$$\mathbf{A}' = \mathbf{F}(\mathbf{A}) ,$$

has a stable time-periodic solution $\mathbf{B}(t) = \mathbf{B}(t + P)$ for some $P > 0$. Thus (13.82) can be thought of as an example of an RD system where diffusion is small, and small also is the effect of localised impurities, represented by the last term on the right of (13.82). We now introduce a slow-time scale T given by $T = \varepsilon t$, and look for solutions of (13.82) of the form

$$\mathbf{A}(\varepsilon, t, \mathbf{x}) = \mathbf{A}^0(t, T, \mathbf{x}) + \varepsilon \mathbf{A}^1(t, T, \mathbf{x}) + \varepsilon^2 \mathbf{A}^2(t, T, \mathbf{x}) + \dots , \tag{13.83}$$

requiring $\mathbf{A}^1, \mathbf{A}^2, \dots$ to be bounded in time. On substituting (13.83) into (13.82) we obtain that $\mathbf{A}^0, \mathbf{A}^1$ should satisfy

$$\frac{\partial \mathbf{A}^0}{\partial t} = \mathbf{F}(\mathbf{A}^0) , \tag{13.84}$$

$$\frac{\partial \mathbf{A}^1}{\partial t} - \mathbf{F}_A(\mathbf{A}^0)\mathbf{A}^1 = -\frac{\partial \mathbf{A}^0}{\partial T} + D \triangle \mathbf{A}^0 + \mathbf{g}(\mathbf{x}, \mathbf{A}^0) , \tag{13.85}$$

where $\mathbf{F}_A(\mathbf{A}^0)$ denotes the jacobian matrix of $\mathbf{F}(\mathbf{A})$ particularised at $\mathbf{A} = \mathbf{A}^0$. Solving (13.84) gives

$$\mathbf{A}^0 = \mathbf{B}(t + \psi(T, \mathbf{x})) , \tag{13.86}$$

where the phase variable $\psi(T, \mathbf{x})$ is to be determined yet. From (13.85) and (13.86) it follows that $\mathbf{A}^1$ has to solve

$$\frac{\partial \mathbf{A}^1}{\partial t} - \mathbf{F}_A(\mathbf{B})\mathbf{A}^1 = -\mathbf{B}' \frac{\partial \psi}{\partial T} + D(\mathbf{B}' \triangle \psi + \mathbf{B}'' |\nabla \psi|^2) + \mathbf{g}(\mathbf{x}, \mathbf{B}) \equiv \mathbf{G}(\psi, \mathbf{x}, t) . \tag{13.87}$$

We are interested in bounded solutions of (13.87). To obtain them, a suitable orthogonality condition has to be imposed concerning the right-hand side there. More precisely, by (13.84) and (13.86), we know that the equation

$$\frac{\partial \mathbf{u}}{\partial t} - \mathbf{F}_A(\mathbf{B}(t + \psi))\mathbf{u} = 0 , \tag{13.88}$$

has a periodic solution $\mathbf{u} = \mathbf{B}'(t + \psi)$. Since we are requiring (13.86) to be a stable solution of (13.84), we need to impose that all solutions of (13.88) which are linearly independent of $\mathbf{B}'(t + \psi)$ should decay exponentially in time. Under these assumptions, there is a unique row vector $\mathbf{z}^T(t + \psi)$ which is periodic with period P, and is such that, for all t

$$\frac{\partial \mathbf{z}^T}{\partial t} + \mathbf{z}^T \mathbf{F}_A(\mathbf{B}(t + \psi)) = 0 , \qquad \mathbf{z}^T(t + \psi)\mathbf{B}'(t + \psi) = 1 .$$

Then a solution of (13.87) is bounded in time if and only if

$$\int_0^P \mathbf{z}^T \mathbf{G}(\psi, \mathbf{x}, s)\, ds = 0 , \tag{13.89}$$

an orthogonality condition. Incidentally, this is precisely the argument that eventually yields Equations (13.79) or (13.81), except that one has to go up to higher-order terms in the corresponding expansion to be analysed in such case (cf. [27] and [51] for details).

From (13.89), using periodicity we eventually obtain that ψ should satisfy

$$\frac{\partial \psi}{\partial T} = D_1(\triangle \psi + \Gamma |\nabla \psi|^2) + \alpha(\mathbf{x}) , \tag{13.90}$$

where

$$\begin{cases} D_1 = \frac{1}{P} \int_0^P \mathbf{z}^T(s) D \mathbf{B}'(s)\, ds , \\ \Gamma = \frac{1}{P} \int_0^P \mathbf{z}^T(s) D \mathbf{B}''(s)\, ds , \\ \alpha(\mathbf{x}) = \frac{1}{P} \int_0^P \mathbf{z}^T(s) \mathbf{g}(\mathbf{x}, \mathbf{B}(s))\, ds . \end{cases} \tag{13.91}$$

Summing all these results up, we have obtained that

$$\mathbf{A}(t, \mathbf{x}) = \mathbf{B}(t + \psi(t, \mathbf{x})) + O(\varepsilon) . \tag{13.92}$$

Equations (13.90) to (13.92) can be thought of as providing a description of a distributed medium consisting in a large population of individual oscillators which are weakly coupled by diffusion, the effect of which consists in introducing a phase shift between different points. In particular, Equation (13.90) provides a law for the evolution in time of that shift. The reader is referred to [51,66–68,82] for the derivation of phase equations under different assumptions, as well as for discussing the phenomenon of synchronisation of coupled oscillators.

Having derived (13.90) to (13.92), we are now in a position to discuss the existence of target patterns for (13.82). A first remarkable fact is that for bounded initial conditions, targets can only exist if $\mathbf{g}(\mathbf{x}, \mathbf{A}) \neq 0$. Indeed, assume on the contrary that $\mathbf{g}(\mathbf{x}, \mathbf{A}) = 0$. Then, by (13.91), $\alpha(\mathbf{x}) = 0$. On setting

$$Z = e^{\Gamma\psi} , \tag{13.93}$$

(13.91) reduces to

$$\frac{\partial Z}{\partial T} = D_1 \triangle Z . \tag{13.94}$$

Therefore the initial value problem for Equation (13.82) can be explicitly solved (cf. formula (13.5)) to give

$$\psi(T, \mathbf{x}) = \frac{1}{\Gamma} \log (4\pi D_1 T)^{-1} \int_{\mathbb{R}^2} \exp \left\{ \frac{\Gamma\psi(0, \mathbf{y}) - |\mathbf{x} - \mathbf{y}|^2}{4D_1 T} \right\} d\mathbf{y} .$$

In particular, if $\psi(0, \mathbf{x})$ is bounded, $\psi(T, \mathbf{x})$ converges to a constant as $T \longrightarrow \infty$, and asymptotically the medium oscillates with uniform phase shift. When $\psi(0, \mathbf{x})$ is unbounded, however, target patterns can be produced (see for instance (13.34) in [26]).

Consider now the case when impurities are present, i.e., $\mathbf{g}(\mathbf{x}, \mathbf{A}) \neq 0$, when $\alpha \neq 0$ in (13.91). Using (13.93), we obtain this time

$$\frac{\partial Z}{\partial T} = D_1 \triangle Z + \Gamma\alpha(\mathbf{x}) Z . \tag{13.95}$$

To solve (13.95), we now separate variables by setting

$$Z(T, \mathbf{x}) = e^{\omega T} \Phi(\mathbf{x}) , \tag{13.96}$$

thus obtaining the following eigenvalue problem: to find Φ and ω such that

$$D_1 \triangle \Phi + \Gamma\alpha(\mathbf{x})\Phi = \omega\Phi , \qquad \Phi(\mathbf{x}) \text{ bounded in } \mathbb{R}^2 . \tag{13.97}$$

To proceed further, we need to introduce additional assumptions on $\alpha(\mathbf{x})$. Basically, we want to solve (13.97) explicitly, and to this end we need $\alpha(\mathbf{x})$ to be a smooth, rapidly decaying function, so that classical spectral theory could be invoked. Assume for instance that $\alpha(\mathbf{x})$ is smooth and compactly supported in a ball $B_R(\mathbf{x}_0) = \{\mathbf{x} : |\mathbf{x} - \mathbf{x}_0| \leq R\}$ for some $\mathbf{x}_0 \in \mathbb{R}^2$ and $R > 0$, and that $\int_{\mathbb{R}^2} \alpha(\mathbf{x})\, d\mathbf{x} > 0$. It is then known (cf. for instance [41,79]) that (13.97) has a finite number $m \geq 1$ of real eigenfunctions $\Phi_1(\mathbf{x}), \cdots, \Phi_m(\mathbf{x})$, which correspond to eigenvalues $\omega_1, \cdots, \omega_m$ such that $\omega_1 > \omega_2 \geq \omega_3 \geq \cdots \geq \omega_m > 0$. Moreover $\Phi_1(\mathbf{x})$ does not change sign. Besides that, there exists a two-dimensional continuum of eigenfunctions $\Phi(\mathbf{k}, \mathbf{x})$. These correspond to eigenvalues $(-D_1|k|^2)$ and are given as the solutions of

$$\Phi(\mathbf{k}, \mathbf{x}) = e^{i\mathbf{k}\cdot\mathbf{x}} + \frac{i\Gamma}{4D_1} \int_{\mathbb{R}^2} H_0^{(1)}(|\mathbf{k}|\,|\mathbf{x} - \mathbf{y}|)\alpha(\mathbf{y})\Phi(\mathbf{k}, \mathbf{y})\, d\mathbf{y} , \tag{13.98}$$

where $H_0^{(1)}$ is the zero-order Hankel function (see [1] for definitions and properties of this special function). Summing up, it follows that the solutions of (13.90) can be represented by means of (13.93), where

$$Z(T, \mathbf{x}) = \beta_1 e^{\omega_1 T}\Phi_1(\mathbf{x}) + \sum_{j=2}^{m} \beta_j e^{\omega_j T}\Phi_j(\mathbf{x}) + H(T, \mathbf{x}) - \sum_{j=1}^{m} \gamma_j(T)\Phi_j(\mathbf{x}) + v(T, \mathbf{x}) , \tag{13.99}$$

and

- $H(T, \mathbf{x})$ is the solution of (13.94), $H(0, \mathbf{x}) = \exp(\Gamma\psi(0, \mathbf{x}))$,
- $\beta_j = (\int_{\mathbb{R}^2} \Phi_j^2(\mathbf{x})\, d\mathbf{x})^{-1} \int_{\mathbb{R}^2} \Phi_j(\mathbf{x}) \exp(\Gamma\psi(0, \mathbf{x}))\, d\mathbf{x}$,
- $\gamma_j(T) = (\int_{\mathbb{R}^2} \Phi_j^2(\mathbf{x})\, d\mathbf{x})^{-1} \int_{\mathbb{R}^2} \Phi_j(\mathbf{x}) H(T, \mathbf{x})\, d\mathbf{x}$ when $1 \leq j \leq m$, and
- $v(T, \mathbf{x})$ is the contribution arising form the continuum spectrum.

(13.100)

Cumbersome as they may appear, these formulae allow for deriving relevant information about the asymptotics of $\Phi(T, \mathbf{x})$. For instance, arguing as in [26] (where suitable estimates on $v(T, \mathbf{x})$ are obtained, and the asymptotic behaviour of eigenfunctions is used), it may be shown that in the region where

$$e^{\omega_1 T - k_1|\mathbf{x} - \mathbf{x}_0|} \ll 1 \quad \text{and} \quad T \gg 1 , \qquad \text{with} \quad k_1 = \left(\frac{\omega_1}{D_1}\right)^{\frac{1}{2}} , \tag{13.101}$$

the function $H(T, \mathbf{x})$ provides the largest contribution in (13.99). One then has that, in such a region

$$\mathbf{A}(T, \mathbf{x}) \sim \mathbf{B}\left(t + \frac{1}{\Gamma}\right) \log H(T, \mathbf{x}) ,$$

and since $H(T, \mathbf{x})$ converges to a constant for large T, it turns out that whenever (13.101) holds the system eventually approaches toward a spatially constant solution. On the other hand, in the region where

$$e^{\omega_1 T - k_1|\mathbf{x} - \mathbf{x}_0|} \gg 1 , \qquad T \gg 1 , \tag{13.102}$$

it is the first term in the right of (13.99) which prevails, and one then has that

$$\mathbf{A}(t, \mathbf{x}) = \mathbf{B}\left((1 + \frac{\varepsilon\omega_1}{\Gamma})t + \frac{1}{\Gamma} \log \Phi_1(\mathbf{x}) + \frac{1}{\Gamma} \log b_1\right) + O(\varepsilon) . \tag{13.103}$$

Since

$$\Phi_1(x) \sim C_1(k_1 r)^{-\frac{1}{2}} e^{-k_1 r} \quad \text{for some} \quad C > 1 \,,$$

and $k_1 r \gg 1$ with $r = |x|$, (13.103) yields a target pattern wave (up to corrections of order $O(\varepsilon)$) which is outgoing for $\Gamma > 0$ and ingoing when $\Gamma < 0$. Notice that the initial value $\psi(0, \mathbf{x})$ enters (13.103) only via the phase shift $\frac{1}{\Gamma} \log \mathfrak{b}_1$.

We conclude by observing that it is possible to perform a similar analysis for impurities $\alpha(\mathbf{x})$ located around two different points $\mathbf{x}_0$ and $\mathbf{x}_1$. Then the precise form of $\alpha(\mathbf{x})$ determines the eigenvalues around $\mathbf{x}_0$ and $\mathbf{x}_1$. In particular, it can be shown that, out of the two emanating targets, it is that having largest first eigenvalues ω_{1i} $(i = 0, 1)$ which eventually takes over. See [26] for details.

13.4 Models of Chemotaxis

In this section we shall deal with some RD systems that have been used to model an important biological activity, namely chemotaxis. By this we refer in general to motion induced by chemical substances, a widely accepted framework to describe the ability of single cells or micro-organisms to sense the direction of external chemical sources, and to migrate towards (or away from) these. Chemotaxis is known to occur in a variety of situations, as for instance during the development of the nervous system, in inflammatory and wound healing responses, and in tumour growth and metastasis, among others. It also plays an important role in the social life of micro-organisms, a subject that will be examined in some detail below. In the following, we shall briefly describe some instances where chemotaxis is a key factor, and will examine some of the mathematical models that have been proposed to provide quantitative and qualitative insight on particular aspects on this phenomenon.

13.4.1 Axon Growth and Neuron Navigation

The nervous system of a person is known to perform a sophisticated set of functions. This requires of a highly complex pattern of wiring among nervous cells (called neurones). The number of these is of the order of 10^{12}, each establishing on average about 10^3 connections (called synaptic contacts) with various targets. Neuronal connections form during embryonic development, when each differentiating neuron sends out an axon, tipped at its leading edge by the growth cone, which migrates through the embryonic environment to meet its target.

Growth cones were first described by Ramón y Cajal in chicken embryos (cf. [73]). These structures are continuously expanding and retracting; this is the way in which growth cones integrate and transduce chemical signals arising from targets and neighbour tissues. In 1893, Ramón y Cajal advanced the so-called chemotactic

hypothesis (cf. [74]), according to which growth cones should be "excitable by substances secreted by some nervous cells," their motion being guided to their eventual targets by "chemical streams." Experimental verification of this conjecture had to wait for a long time; see [83] and [80] for surveys of the aspects involved.

Much is already known about the manner in which neuron navigation occurs. For instance, as explained in [83], axon trajectories appear to be broken into short segments. In this way, reaching a distant target is split into many simpler (and shorter) steps, which all together allow axons to move over comparatively large distances (usually on the order of centimetres, that is, over a thousand times the diameter of each cell body). A second feature stressed in [83] is that the wiring of the nervous system takes place in a stepwise manner. This means that the first axons that develop have to move within an axon-free environment. However, later moving ones have to deal with an expanding media where earlier sailing cells make up a scaffolding network where others should travel along.

Even if large journeys can be broken into shorter legs, the question remains of understanding how each axon navigates any short segment. As described in [83], axons seem to respond to the coordinate action of four types of guidance cues: attractive and repulsive, which can be either short-range or long-range. Long-range attraction and repulsion seem in turn to be produced by diffusible factors, whereas short-range guidance appears to be provided by contact-mediated mechanisms, involving nondiffusible cell surface and extracellular matrix (ECM) molecules. We next proceed to remark on some modelling aspects of long-range, diffusive attraction, or repulsion.

13.4.1.1 Sensitivity, Adaptation, Amplification

A first modelling approach might consist in considering each biological unit (axons in the case recalled above, but possibly lymphocytes or amoebae in the situations to be considered later) as a black box, from which some robust properties are to be expected, irrespective of the precise way in which these are achieved. For instance, for long-range guidance based on the detection of chemotactic gradients to be successful, the organisms involved are expected to fulfill some requirements, namely:

- To be able to respond reliably to small gradients of guidance cues across their surface (sensitivity)
- As migration takes place in a medium where the basal concentration of chemical signals varies by several orders of magnitude, organisms need to constantly re-adjust their sensitivity, a process usually termed as adaptation.

Besides that, in a living environment the detection-orientation system has to allow for high-gain persistent, polarised signalling in response to chemoattractant gradients (amplification).

As a matter of fact, experiments reported in [62] show that under exposure to high levels of netrin-1 of brain-derived neurothropic factor (BDNF), growth cones

of cultured *xenopus* spinal neurones undergo consecutive phases of desensitisation and resensitisation (that is, adaptation) in their ability to detect gradients of netrin-1 of BDNF. Moreover, these cyclic phases o f desensitisation and resensitisation are reflected in the zigzag path of alternating attractive and repulsive turning of advancing growth cones towards their source of chemoattractant. However, in the absence of guidance factor, no such type of path is observed, and the growth cone advances in an irregular and unpredictable manner.

A model of amplification in growth cones has been proposed in [60]. It consists in a system of ordinary differential equations involving three variables: a saturating, self-enhancing activator, coupled with two antagonistic equations. Of these, one equilibrates rapidly over the whole cell, causing competition among different surface elements, which is won by those exposed to the highest concentration of external cues. A second antagonistic reaction is assumed to act locally. It has a longer time constant, and produces destabilisation of peaks after they have formed. On the other hand, a model for adaptation different from (but also motivated by) the activator-inhibitor models of [58–60] has recently been proposed in [50,54]. Again, three variables are considered: a response element that can be active (denoted by R^*) or inactive, its total concentration being R_0, and an active excitory (A^*) and inhibitory (I^*) enzymes that catalyse the activation and inactivation of the system. Activation is in turn regulated by receptor occupancy in the cell membrane, which is proportional to the concentration of the local signalling molecule (S). The corresponding set of equations is

$$\begin{cases} \dfrac{\mathrm{d}R^*}{\mathrm{d}t} = -k_1 R^*(t) I^*(t) + k_2 (R_0 - R^*(t)) A^*(t) \,, \\ \dfrac{\mathrm{d}I^*}{\mathrm{d}t} = -k_3 I^*(t) + k_4 (I_0 - I^*(t)) S \,, \\ \dfrac{\mathrm{d}A^*}{\mathrm{d}t} = -k_5 A^*(t) + k_6 (A_0 - A^*(t)) S \,, \end{cases} \tag{13.104}$$

where letter k with different subscripts is used to denote the kinetic constants of the various reactions involved. Assuming the presence in (13.104) of some small parameters, asymptotic limits are identified in [50,54] for which, as $t \longrightarrow \infty$

$$\frac{R^*}{R_0} \sim C \frac{A_0}{I_0} \qquad \text{for some } C > 0 \text{ independent of } S \,,$$

so that R^* will not depend on the signalling molecule concentration, whence the system will exhibit the adaptation property.

It has been already mentioned that signal processing within the cell is mediated by receptor occupancy at its membrane. In other words, the incoming external cue is captured at some particular places (receptors) scattered over the cell boundary, thus triggering an internal signalling cascade. The physical mechanism by which growth cones sense gradients is a subject deserving considerable attention, and one in which more needs to be known. For instance, in a situation as that of a cell, in which the

energy due to thermal fluctuations is large enough to change the cell motion, the question naturally arises of what are the physical limitations on a cell's ability to sense and respond to changes in its environment. This issue was addressed in the work [5], where a model was produced that provided estimates for the statistical fluctuations in the measuring of concentrations by a small sensing device. From that model, the authors obtained estimates on sensitivity with respect to various factors including a bound on the minimum detectable gradient. This study has been recently taken up in [23], where comparison with experiments and limitations on its predictive value are discussed in detail.

We conclude this section by remarking on a macroscopic, RD-model for axon guidance. Here target cells and growth cones are represented as points in a two- or three-dimensional space, and attention is paid to the change in the concentrations of various chemical signals. More precisely, let us follow [32] and consider the interaction of three types of diffusible substances:

- A chemoattractant u_1 that is released by target cells at a rate σ_1 and has diffusion coefficient D_1
- A chemoattractant u_2 released by the axonal growth cones at a rate σ_2, with diffusion constant D_2
- A chemorepellent u_3 secreted by the axonal growth cones at a rate σ_3 which diffuses with a coefficient D_3

Here we are also denoting by u_1, u_2, and u_3 the concentrations of the signals involved. Assuming that axon growth occurs on a much longer scale than the time needed for diffusive fields to equilibrate (again, a small-parameter hypothesis), the authors of [32] arrive at the following system

$$\begin{cases} \triangle \rho_2 - k_2^2 u_2 = -\dfrac{\sigma_2}{D_2} \displaystyle\sum_\alpha \delta(x - r_\alpha(t)) \,, \\ \triangle \rho_1 - k_1^2 u_1 = -\dfrac{\sigma_1}{D_1} \displaystyle\sum_i \delta(x - x_i) \,, \\ \triangle \rho_3 - k_3^2 u_3 = -\displaystyle\sum_\alpha \sigma_3 \delta(x - r_\alpha(t)) \,, \end{cases} \tag{13.105}$$

where x_i is the fixed position of target cell i, r_α is the location of the α^{th}-growth cone at time t, k_i ($1 \leq i \leq 3$) is the inverse diffusive length of chemical u_i, and $\delta(x - s)$ denotes Dirac's delta at $x = s$. We refer to [32] for a numerical study of the phenomena of bundling (during navigation) and debundling (on approaching the target). Actually, the analysis made in [32] is concerned with a number of situations, involving not only diffusible signals but also contact interactions, but we shall omit further details here.

13.4.2 Aggregation in Slime Moulds: the Keller-Segel System

The second problem in this section is concerned with morphogenesis, a key feature in the development of multicellular organisms, and already an inspiring motivation behind Turing's seminal work [84]. One of the simplest aspects of morphogenesis is cell aggregation. Indeed, as observed in [65], "... Aggregation phenomena, in which spatially separated cells gather together, form a multicellular group and then proceed to differentiation, are perhaps ideal for studying interactions between cells during morphogenesis. Unfortunately, not many systems are known in which aggregation occurs clearly separated in time from differentiation. Among other reasons, this makes it particularly important to make a detail study of the one *in vivo* system that is well characterised, namely the cellular slime moulds."

The precise biological features of these organisms which are of interest here are succinctly summarised by Bonner ([9], p.62 ; see also [8]) as follows: "... Cellular slime moulds are soil amoebae. They feed as separate individuals on bacteria, and after they have finished the food supply, they stream together to central collection points to form a multicellular individual of thousands of cells. This mass of amoebae moves as a unified "slug" toward light and is also oriented by heat gradients. After this period of migration, the anterior cells turn into stable cells that keep piling onto the tip, while most of the posterior cells turn into spores. The spore mass is slowly lifted into the air as the stalk elongates; the final result is a small fruiting body, in the order of one or two millimetres high, in which a spherical spore mass is supported on a slender stalk made up of large, vacuolate, dead stalk cells ...."

Out of all biological aspects mentioned above, each of which has interest on its own, we shall focus here on aggregation toward "central collection points." More precisely, it is known that when food becomes scarce, some individuals start emitting pulses of a chemical (cAMP $\equiv$ cyclic aminophosphatase in the case of the mould Dictyostellium discoideum, Dd for short). Organisms then proceed to move towards higher concentrations of the substance thus produced, and eventually concentrate into lumps. In the course of motion, experiments reveal a variety of structures: target and spiral waves (of which we have discussed before), but also streaming patterns.

We shall examine now an early continuum model which intends to describe this aggregation stage. It was introduced in 1970 by Keller and Segel (cf. [47]) and, in its simplest version, only two variables are considered. These are the concentration of cells at any point x and time t, to be denoted by $u(x,t)$, and that of the chemical producing aggregation, represented by $v(x,t)$. The conservation equations for $u(x,t)$ and $v(x,t)$ are of the form

$$\begin{aligned} \frac{\partial u}{\partial t} &= -\nabla \cdot \mathbf{J}_u \,, \\ \frac{\partial v}{\partial t} &= -\nabla \cdot \mathbf{J}_v + Au - Bv \,, \qquad A>0\,,\ B>0\,, \end{aligned} \tag{13.106}$$

where $\mathbf{J}_u$ and $\mathbf{J}_v$ are respectively the fluxes of cell and chemical concentrations,

and terms Au and $(-Bv)$ are particularly simple choices corresponding to chemical production and decay. As to the fluxes, these are assumed to be given by

$$\mathbf{J}_v = -D_v \nabla v \,, \qquad \mathbf{J}_u = -D_u \nabla u + u \nabla \chi(v) \,. \tag{13.107}$$

Here the diffusion coefficients D_u, D_v are positive, and $\chi(v)$ is the so-called chemotactic function, whose gradient attracts cells to gather together. A simple choice is to assume it to be linear, $\chi(v) = \chi v$ for some $\chi > 0$. Putting all pieces together, we eventually arrive at

$$\begin{cases} \dfrac{\partial u}{\partial t} = D_u \Delta u - \chi \nabla \cdot (u \nabla v) \,, \\[2ex] \dfrac{\partial v}{\partial t} = D_v \Delta v + Au - Bv \,. \end{cases} \tag{13.108}$$

Equations (13.108) are to be considered in a domain (usually bounded) $\Omega \subset \mathbb{R}^N$. Natural choices for N are $N = 2$ (a reasonable approximation for a Petri dish) and $N = 3$. For the purpose of mathematical analysis, (13.108) has to be supplemented with suitable initial and boundary conditions.

In the case of bounded domains, it is often assumed that there is no flux at the boundary, i.e.,

$$\frac{\partial u}{\partial \mathbf{n}} = \frac{\partial v}{\partial \mathbf{n}} = 0 \qquad \text{for } \mathbf{x} \in \partial\Omega \quad \text{and} \quad t > 0 \,. \tag{13.109}$$

Systems akin to (13.108) can be derived from an interacting stochastic system consisting of many particles, under the assumption that such interaction is of a moderate character when the population size increases to infinity; cf. [81] and also [38,71] for details concerning this derivation.

In the sequel we shall follow [34] to describe some properties of (13.108), a system that despite its simplicity encodes a rich structure. To begin with, one may wonder if the formation of dense cell aggregates (often referred to as chemotactic collapse) is captured at all in the model (13.108). In mathematical terms, this question may be formulated as follows:

Does system (13.108) possess solutions $(u(\mathbf{x},t), v(\mathbf{x},t))$ such that $u(\mathbf{x},t)$ converges to some Dirac mass in finite time, i.e., such that

$$u(\mathbf{x},t) \longrightarrow M\delta(\mathbf{x} - \mathbf{x}_0) \qquad \text{as} \qquad t \longrightarrow T \,, \tag{13.110}$$

for some $\mathbf{x}_0 \in \Omega$, $T < +\infty$ and $M > 0$?

In this approach, aggregation is represented as a type of blow-up, considered to be the late stage of an instability arising of an initially homogeneous state. As a matter of fact, this early stage can be analysed by means of the techniques recalled in section 13.2.5. To begin with, one has that $u(x,t) = u_0$ and $v(x,t) = v_0$ are constant solutions of (13.108) provided that $Au_0 = Bv_0$. Assume now that $N = 2$ for definiteness, and let us try on (13.108) an expansion of the form

$$u(x,y,t) = u_0 + a\cos(q_1 x + q_2 y)e^{\sigma t} + \cdots ,$$
$$v(x,y,t) = v_0 + b\cos(q_1 x + q_2 y)e^{\sigma t} + \cdots , \qquad (13.111)$$

where the constants a, b, q_1, and q_2 are to be determined. Retaining only linear terms, Equation (13.108) may be replaced in a neighbourhood of (u_0, v_0) by

$$\begin{cases} \dfrac{\partial u}{\partial t} = D_u \triangle u - \chi u_0 \triangle v , \\ \dfrac{\partial v}{\partial t} = D_v \triangle v + Au - Bv . \end{cases} \qquad (13.112)$$

Plugging (13.111) into (13.112) eventually yields

$$\chi u_0 q^2 b - (\sigma + q^2 D_u)a = 0 \quad , \; q^2 = q_1^2 + q_2^2 ,$$
$$-(q^2 D_v + B + \sigma)b + Aa = 0 ,$$

a dispersion relation similar to (but more involved than) (13.9). Since we are interested in nontrivial values of a and b, we need to impose

$$\sigma^2 + \sigma(q^2(D_u + D_v) + B) + q^2(D_u(q^2 D_v + B) - \chi u_0 A) = 0 . \qquad (13.113)$$

It is readily seen that a positive solution of this quadratic equation exists only if

$$0 < q^2 < (\chi u_0 A - BD_u)(D_u D_v)^{-1} ,$$

which in turn requires

$$\frac{\chi A u_0}{BD_u} > 1 . \qquad (13.114)$$

Actually, condition (13.114) implies that homogeneous steady states become (linearly) unstable whenever the initial concentration of cells is large enough.

When (13.113) holds, there exists a continuum of values of q for which (13.114) is satisfied. In particular, there is a value q^* at which the positive root $\sigma = \sigma(q^2)$ of (13.113) achieves a maximum.

Assuming $0 < q^2 \ll 1$, an approximate plot of σ against q^2 can be obtained as shown in Figure 13.7.

The argument just sketched provides a reasonable description of the initial stages of aggregation, that may be considered to be triggered by random perturbations (biological noise) around a given homogeneous state. However, it clearly appears that chemotactic collapse cannot be fully accounted for in such way. Indeed, the validity of this approach is confined to regions where perturbations remain small. As remarked in [65], it cannot be excluded that, after an initial period of

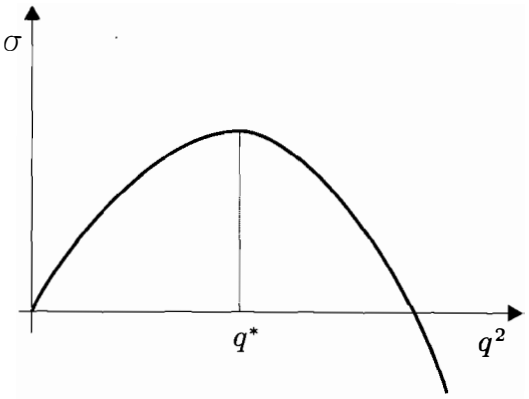

Figure 13.7
The relation between $\sigma(q^2)$ and q^2 for $0 < q^2 \ll 1$.

growth, the system would "settle down to another stationary state, spatially nonuniform, but far from aggregate." After all, this is precisely what was expected from the activator-inhibitor systems mentioned in section 13.2.6. Furthermore, even if some fluctuations would produce solutions that never return to a quiescent state, they could do so in infinite time, or even if blowing up in a finite time, they could do so in a different manner than that prescribed by (13.110).

We now provide a quick overview of known results concerning aggregation properties of system (13.108). As a startpoint, it was shown in [42] that in space dimension $N = 2$, solutions of (13.108), (13.109) exist for all times if the initial density $\bar{u}_0 = |\Omega|^{-1} \int_\Omega u_0(x)\,dx$ is small enough. However, radial solutions corresponding to $\bar{u}_0$ sufficiently large blow up in finite time. The existence of a critical threshold on $\bar{u}_0$ (that can be precisely characterised, see [64]) for blow up to occur is a relevant feature of the two-dimensional case, which is known to be absent when $N = 3$ (see [6] and [33] for results in that direction).

The actual occurrence of chemotactic collapse for radial solutions when $N = 2$ has been shown in [35] (for a simplified version of (13.108) corresponding to the case $0 < D_u \ll D_v$) and in [36,37] (for the general system (13.108) with both diffusion coefficients of order one). The structure of the solution which eventually unfolds into a Dirac's delta is better obtained by asymptotic methods. The basic idea consists in considering separately an inner region, located in a thin layer around the blow-up point (say, x_0), and an external, outer region, where solutions change slowly in time. At the inner region, the solution converges (in rescaled variables) toward a stationary solution of (13.108); the (*a priori* unknown) radius $R(t)$ of this region enters in the form of the scaling required for the stationary solution to eventually form there. At the outer region, our solution can be safely approximated by that of a linearised problem, where all information emanating from the inner region is averaged out in the form of a lumped source term. The radius $R(t)$ is then obtained

by requiring these two approximations (inner and outer) to match at an intermediate region, which overlaps with the inner and outer ones. We refer to [34] for additional details on this strategy, which is fully carried out in references [35–37].

We conclude this section by further remarking on some interesting properties of system (13.108). To begin with, when $N = 3$ a different blow-up mechanism appears. It consists in an imploding, smoothed out shock wave moving towards the blow-up point (cf. [33]). On the other hand, the stability of the chemotactic collapse obtained when $N = 2$ has been extensively discussed in [86], whereas possible regularisations of (13.108) allowing for solutions to be continued beyond blow-up (a natural requirement from a biological point of view) are studied in [87,88]. We also refer to these last two papers for recent mathematical analysis on the Keller-Segel model.

13.4.3 Modelling Some Aspects of Chemotaxis

The previous section was concerned with describing aggregation in slime moulds from a macroscopic point of view. In this way, cells were represented as points, and their individual evolution was reduced to the analysis of their concentration and that of the chemical released during clustering.

While such a crude simplification may be relevant in some contexts, it is far from being realistic in others. In particular, every aspect of the sophisticated processes associated to signal capturing by surface receptors, and its subsequent transduction to trigger a motile response in the cell, were simply ignored. Although these issues are far from being completely elucidated to this day, models have been proposed that partially account for these features. To keep this work within reasonable bounds, only two of them will be briefly described below. In particular, the underlying (and challenging) question of elaborating a comprehensive, multiscale model for Dd will not be addressed here.

The first work to be succinctly commented in the sequel is that by Hagan and Cohen (cf. [28]). Their goal consisted in providing a RD scenario for regulation of cAMP in Dd. They assumed that this can be accounted for in terms of the following variables: the extracellular (resp. intracellular) concentration of cAMP, the intracellular concentration of an inhibitor, and a lumped variable representing concentration of intracellular stored reserves. These are respectively denoted by $\alpha(x,t)$, (resp. $\bar{A}$), C, and S. The interplay of these variables is described in [28] by means of the following system

$$\begin{cases} \dfrac{\partial \alpha}{\partial t} = \bar{q}\bar{l}\bar{A} - p\alpha + D\Delta\alpha\,, \\ \dfrac{\partial \bar{A}}{\partial t} = \bar{f}(\alpha, C) - \bar{l}\bar{A}\,, \\ \dfrac{\partial C}{\partial t} = k(\alpha)S - a(C) - b(C)\,, \\ \dfrac{\partial S}{\partial t} = \dfrac{1}{n}[-k(\alpha)S + a(C)]\,. \end{cases} \tag{13.115}$$

Let us remark briefly on the various terms appearing in (13.115). The first equation therein describes changes in space and time of the concentration of external cAMP. This last increases proportionally (with factor $\bar{q}$) to the rate $\bar{l}\bar{A}$ at which internal cAMP is secreted by the cells. The second and third terms on the right account respectively for degradation and diffusion. The second equation represents synthesis of internal cAMP, and its loss by leaking to the external environment. Activation is due to function $f(\bar{\alpha}, C)$ which is increasing in α, and inhibited by C, so that it eventually saturates in a sigmoid manner (cf. Figure 1 in [28]). The third equation in (13.115) accounts for production of a feedback inhibitor C by catabolism of the stored reserves S (at a α-dependent rate, $k(\alpha)$). C is also recycled (at a rate $a(C)$) to rebuild S, and is lost at a rate $b(C)$. Finally, the last equation describes consumption of the stored reserves S at a rate $(\frac{1}{n})$ times the net production rate of C, and its simultaneous restoring (already discussed).

Of particular importance is the fact that n represents the number of monomers in one polymeric unit of S, so that $n \gg 1$, and we already have a small parameter in (13.115). As pointed out in [28], use of experimental information allows for further separation of scales in the model. For instance, degradation of α is rapid (between $\frac{1}{2}$ and 2 seconds), which suggests setting $p = \frac{1}{\varepsilon}$ with $0 < \varepsilon \ll 1$. Production of intracellular cAMP seems also to be fairly rapid (about 15 seconds). On the other hand, production of inhibitor occurs at a much slower pace (about 100 seconds). Furthermore, since $n \gg 1$, S is depleted only in a very slow scale (of the order of hours). Thus, on setting $ql = \varepsilon\bar{q}\bar{l}$, $\delta\bar{f}(\alpha, C) = f(\alpha, C)$, $l = \delta\bar{l}$ with $0 < \varepsilon \ll \delta \ll 1$, (13.115) can be recast in the form

$$\begin{cases} \dfrac{\partial \alpha}{\partial t} = \dfrac{1}{\varepsilon}(ql\bar{A}\alpha) + D\Delta\alpha\,, \\ \dfrac{\partial \bar{A}}{\partial t} = \dfrac{1}{\delta}(f(\alpha, C) - l\bar{A})\,, \\ \dfrac{\partial C}{\partial t} = k(\alpha)S - a(C) - b(C)\,, \\ \dfrac{\partial S}{\partial t} = \dfrac{1}{n}[-k(\alpha)S + a(C)]\,. \end{cases} \tag{13.116}$$

One then may argue as follows. Since α evolves in a faster time scale than $\bar{A}$, it is always near equilibrium with $\bar{A}$, so that $\alpha \sim ql\bar{A}$. From the first equation in (13.116) we then obtain that

$$\alpha = ql\bar{A} + \varepsilon\left(D\triangle\alpha - \frac{\partial\alpha}{\partial t}\right) \sim ql\bar{A} + \varepsilon\left(D\triangle(ql\bar{A}) - ql\frac{\partial\bar{A}}{\partial t}\right)$$
$$\sim ql\left(\bar{A} + \varepsilon(D\triangle\bar{A} - \bar{A})\right) . \qquad (13.117)$$

We next consider the second equation in (13.116) and set there

$$A = ql\bar{A} \quad , \quad F(\alpha, C) = qlf(\alpha, C) .$$

Taking advantage of (13.117) and using Taylor's expansion on $F(\alpha, C)$, we obtain

$$\delta\frac{\mathrm{d}A}{\mathrm{d}t} = F(\alpha, C) - lA \qquad (13.118)$$
$$= F(A, C) - lA - \frac{\varepsilon}{\delta}F_A(A, C)\left(F(A, C) - lA\right) + \varepsilon DF_A(A, C)\triangle A + \dots .$$

Arguing in a similar way for the third equation in (13.116), we are able to reduce the original system (13.115) to one consisting of three equations, namely

$$\begin{cases} \delta\dfrac{\partial\bar{A}}{\partial t} = F(A, C) - lA + \varepsilon DF_A(A, C)\triangle A , \\ \dfrac{\partial C}{\partial t} = k(A)S - a(C) - b(C) + \varepsilon DSk'(A)\triangle A , \\ \dfrac{\partial S}{\partial t} = \dfrac{1}{n}[-k(A)S + a(C)] . \end{cases} \qquad (13.119)$$

Moreover, since S changes little in time, we may consider (13.119) as consisting essentially of its first two equations, and having a slowly varying parameter there. The reduced system thus obtained can be analysed in two steps. First, we may drop the (small) diffusivity terms, and then consider the ODE system thereby obtained. Keeping track of the variation of S, it is then possible to classify the corresponding equilibrium states and describe the resulting dynamics in phase space. At a second stage, we introduce back the weak coupling due to diffusion, to characterise the onset of pulse and spiral patterns in the reduced system (13.119) (cf. [28], p. 885-898).

A question also addressed in [28] is the need of a rule connecting external cAMP concentration with cell motion. This is assumed to be that cells move in the direction opposite to cAMP wave propagation. In this way, evidence for the formation of streams can be obtained in the following manner. Suppose that cells are migrating toward a distant aggregation centre located on the x-axis. We can then write A and C in the form

$$\begin{cases} A(t, x) = \widetilde{A}(\omega_0 t + \psi(\tau, x), S_0) + \dots , \quad \tau = \varepsilon t , \\ C(x, t) = \widetilde{C}(\omega_0 t + \psi(\tau, x), S_0) + \dots , \end{cases} \qquad (13.120)$$

(recall Equations (13.82) to (13.90) in the previous section). Here $\psi(\tau, x)$ is the phase shift, that may be assumed to be in the form of a plane wave near the origin: $\psi \sim kx + \gamma\tau$ for some k, γ; w_0 is the average of $\omega(S(x))$, a frequency determined by the local value of $\omega(S(x))$, and S_0 is the average value of $S(x)$. Assuming $\omega(S(x))$ to be almost constant and equal to ω_0 except in a small region: $x^2 + y^2 < r_0^2$, we may write $\psi(\tau, x)$ in the form

$$\psi(\tau, x) = kx + \gamma\tau + P(\tau, x, y) , \qquad (13.121)$$

where P represents the perturbation caused by the inhomogeneities of $\omega(S(x))$ around the origin. From Equations (13.119) to (13.121), it is possible to estimate the term $(\nabla\psi - (k, 0))$ which represents the relative direction field of the cell motion, to eventually produce a streaming pattern as that in Figure 8 in [28].

We conclude this section by succinctly describing a model containing elements already incorporated in [28] together with the explicit consideration of a (possibly large) population of moving organisms, as in the system studied in [32] and recalled in section 13.3.1. More precisely, we follow [70] and consider a family of n organisms, assumed to be approximately circular, moving on a two-dimensional space. The position of any cell is then characterised by the location of its centre, $R_i(t) = (x_i(t), y_i(t)) \equiv r_i(t)$ with $1 \le i \le n$. The model in [70] describes Dd cells which can produce cAMP and move towards a cAMP gradient according to the following rules: Dd cells have membrane receptors that can be either active or inactive. In the active state, the receptors can bind external cAMP, thereby stimulating the synthesis of cAMP inside the cell. This intracellular cAMP is then leaked outside the cell, where it stimulates cAMP receptors, thereby closing a feedback loop. On the other hand, receptors become inactive as a result of prolonged exposure to high cAMP concentrations, which allows for refractory periods in the cell. In mathematical terms, we introduce three variables: $\rho(r, t)$ (fraction of cAMP receptors in active state), $\beta(r, t)$ (concentration of intracellular cAMP), and $\gamma(r, t)$ (concentration of extracellular cAMP) and state the following relations among them

$$\begin{cases} \varepsilon_1\dfrac{\partial\rho}{\partial t} = (-f_1(\gamma)\rho + f_2(\gamma)(1 - \rho))\displaystyle\sum_{i=1}^{n}\delta(r - R_i(t)) , \\ \varepsilon_2\dfrac{\partial\beta}{\partial t} = (s_1\Phi(\rho, \gamma) - \beta(r, t))\displaystyle\sum_{i=1}^{n}\delta(r - R_i(t)) , \\ \dfrac{\partial\gamma}{\partial t} = D\triangle\gamma + \dfrac{1}{\varepsilon_3}(s_2\beta - \gamma)\displaystyle\sum_{i=1}^{n}\delta(r - R_i(t)) . \end{cases} \qquad (13.122)$$

Here functions f_1, f_2, and Φ are given, and a number of parameters appear which allow for separation of scales in suitable asymptotic limits. For instance, arguments are given in [70] to assume that the second equation in (13.122) is in a

quasi-steady state (that is, the internal cAMP dynamics are very fast). Then (13.122) can be reduced to

$$\begin{cases} \varepsilon_1 \dfrac{\partial \rho}{\partial t} = (-f_1(\gamma)\rho + f_2(\gamma)(1-\rho)) \displaystyle\sum_{i=1}^{n} \delta(r - R_i(t)) \,, \\ \dfrac{\partial \gamma}{\partial t} = D\Delta\gamma + \dfrac{1}{\varepsilon_3}(s\Phi - \gamma) \displaystyle\sum_{i=1}^{n} \delta(r - R_i(t)) \,. \end{cases} \tag{13.123}$$

As in the case previously examined (cf. [28]), a locomotion rule needs yet to be added to (13.123) to account for cell motion. Some choices for such rules are discussed in [70], but to give merely a glimpse of the problems therein considered, we just comment on one of these. Let $\mu = \mu(\rho, \gamma)$ be such that $\mu = 0$ if the following conditions are met: either $\rho < \rho_0$ for some critical value ρ_0, or $|\nabla\gamma| < \theta_0$ for some $\theta_0 > 0$; we take $\mu = 1$ otherwise. Then motion of the cells can be described by the equation

$$\frac{\mathrm{d}R_i}{\mathrm{d}t} = \mu \frac{\nabla\gamma}{|\nabla\gamma|} \,, \qquad \text{for } i = 1, \ldots, n \,. \tag{13.124}$$

The mathematical analysis of (13.123), (13.124) with $n \gg 1$ is rather involved. However, numerical simulations seem to be comparatively easier. A number of them were performed in [70], which show occurrence of various types of patterns, including stream formation and spiral motion, in suitable ranges of the parameters appearing in (13.123), (13.124).

13.5 References

[1] Abramowitz, M. and Stegun, I.A., *Handbook of Mathematical Functions*, Dover, New York, 1972.

[2] Andreucci, D., Herrero, M.A., and Velázquez, J.J.L., On the growth of filamentary structures in planar media, Preprint, 2002.

[3] Aronson, D.G., The porous medium equation, in *Nonlinear Diffusion Processes*, A. Fasano and M. Primicerio, Eds., Springer Lecture Notes in Mathematics n° 1224, 1-46, Heidelberg, 1985.

[4] Bender, C.M. and Orszag, S.A., *Advanced Mathematical Methods for Scientists and Engineers*, Springer Verlag, Heidelberg, 1999.

[5] Berg, H.C. and Purcell, E.M., Physics of chemoreception, *Biophysical J.* 20, 193-219, 1977.

[6] Biler, P., Local and global solvability of some parabolic systems modelling chemotaxis, *Adv. Math. Sci. Appl.* 8, 297-308, 1998.

[7] Birkhoff, G. and Rota, G.C., *Ordinary Differential Equations*, John Wiley & Sons, New York, 1989.

[8] Bonner, J.T., *The Cellular Slime Molds*, Princeton Univ. Press, Princeton, NJ, 1967.

[9] Bonner, J.T., *Sixty Years of Biology*, Princeton Univ. Press, Princeton, NJ, 1996.

[10] Casten, R.G., Cohen, H., and Lagerstrom, P.A., Perturbation analysis of an approximation to the Hodgkin-Huxley theory, *Quart. Appl. Math.* Vol. XXXII, 4, 365-402, 1975.

[11] Chandrasekhar, S., Stochastic problems in physics and astronomy, *Rev. Modern Physics* 15, 1-85, 1943.

[12] Coddington, E.A. and Levinson, N., *Theory of Ordinary Differential Equations*, McGraw-Hill, New York, 1995.

[13] Cohen, D.S., Neu, J.C., and Rosales, R.R., Rotating spiral wave solutions of reaction-diffusion equations, *SIAM J. Appl. Math.* 35, 536-547, 1978.

[14] Conway, E., Hoff, D., and Smoller, J., Large time behaviour of solutions of systems of nonlinear reaction-diffusion equations, *SIAM J. Appl. Math.* 35, 1-16, 1978.

[15] Cronin, J., *Mathematical Aspects of Hodgkin-Huxley Neural Theory*, Cambridge University Press, London, New York, 1987.

[16] Cross, M.C. and Hohenberg, P.C., Pattern formation outside of equilibrium, *Rev. Modern Physics* 65, 854-1090, 1993.

[17] Fife, P.C., *Mathematical Aspects of Reacting and Diffusing Systems*, Springer Lecture Notes in Biomathematics n° 28, Heidelberg, 1979.

[18] Fife, P.C. and McLeod, J.B., The approach of solutions of nonlinear diffusion equations to travelling front solutions, *Arch. Rat. Mech. Anal.* 65, 335-361, 1977.

[19] Fife, P.D. and McLeod, J.B., A phase plane discussion of convergence to travelling fronts for nonlinear diffusion, *Arch. Rat. Mech. Anal.* 75, 281-314, 1981.

[20] Fisher, R.S., *The Genetical Theory of Natural Selection*, Oxford University Press, Oxford, 1930.

[21] Friedman, A., *Partial Differential Equations of Parabolic Type*, Robert Krieger Co., Malabar, FL, 1983.

[22] Gierer, A. and Meinhardt, H., A theory of biological pattern formation, *Kybernetik* 12, 30-39, 1972.

[23] Goodhill, G.J. and Urbach, J.S., Theoretical analysis of gradient detection by growth cones, *J. Neurobiol.* 41, 230-241, 1999.

[24] Grimmet, G. and Stirzaker, D., *Probability and Random Processes*, Oxford University Press, Oxford, 2001.

[25] Grindrod, P., *Patterns and Waves*, Oxford University Press, Oxford, 1991.

[26] Hagan, P.S., Target patterns in reaction-diffusion systems, *Adv. in Appl. Math.* 2, 400-416, 1981.

[27] Hagan, P.S., Spiral waves in reaction-diffusion equations, *SIAM J. Appl. Math.* 42, 762-786, 1982.

[28] Hagan, P.S. and Cohen, M.S., Diffusion induced morphogenesis in the development of Dictyostellium, *J. Theor. Biol.* 93, 881-908, 1981.

[29] Hairer, E. and Wanner, G., *Analysis by Its History*, Springer, Heidelberg, 1996.

[30] Hellwig, G., *Partial Differential Equations*, Teubner, Stuttgart, 1977.

[31] Henry, D., *Geometric Theory of Semilinear Parabolic Equations*, Springer Lecture Notes in Mathematics 840, Heidelberg, 1981.

[32] Hentschel, H.G.E. and van Ooyen, A., Models of axon guidance and bundling during development, *Proc. R. Soc. London B*, 266, 2231-2238, 1999.

[33] Herrero, M.A., Medina, E., and Velázquez, J.J.L., Finite-time aggregation into a single point in a reaction-diffusion system, *Nonlinearity* 10, 1754-1793, 1997.

[34] Herrero, M.A., Asymptotic properties of reaction-diffusion systems modelling chemotaxis, in *Applied and Industrial Mathematics*, R. Spigler, Ed., Kluwer Acad. Pub., Dortrecht, 89-108, 2000.

[35] Herrero, M.A. and Velázquez, J.J.L., Singularity patterns in a chemotaxis model, *Math. Ann.* 306, 583-623, 1996.

[36] Herrero, M.A. and Velázquez, J.J.L., Chemotactic collapse for the Keller-Segel model, *J. Math. Biol.* 35, 177-196, 1996.

[37] Herrero, M.A. and Velázquez, J.J.L., A blow-up mechanism for a chemotactic model, *Ann. Scuola Norm. Sup. Pisa, Ser. IV*, vol. XXIV, 633-683, 1997.

[38] Hillen, T. and Othmer, H.G., The diffusion limit of transport equations derived from velocity-jump processes, *SIAM J. Appl. Math.* 61, 751-775, 2000.

[39] Hodgkin, A.L. and Huxley, A.F., A quantitative description of membrane current and its application to conduction and excitation in nerve, *J. Physiology (London)* 117, 500-544, 1952.

[40] Hoel, P.G., Port, S.C., and Stone, C.J., *Introduction to Stochastic Processes*, Houghton Mifflin Co., Boston, 1972.

[41] Ikebe, T., Eigenfunction expansions associated with the Schrödinger operators and their applications to scattering theory, *Arch. Rat. Mech. Anal.* 5, 1-34, 1960.

[42] Jäger, W. and Luckhaus, S., On explosions of solutions to a system of partial differential equations modeling chemotaxis, *Trans. Amer. Math. Soc.* 329, 819-824, 1992.

[43] Jones, C.K.R.T., Stability of the travelling wave solution of the FitzHugh-Nagumo system, *Trans. Amer. Math. Soc.* 286, 431-469, 1984.

[44] Kanel, Y.I., On the stabilization of solutions of the Cauchy problem for equations arising in the theory of combustion, *Mat. Sbornik* 59, 245-288, 1962. See also *Sov. Math. Dokl.* 1, 513-516, 1960, and *Sov. Math. Dokl.* 2, 48-51, 1961.

[45] Keener, J.P., Waves in excitable media, *SIAM J. Appl. Math.* 39, 528-548, 1980.

[46] Keener, J.P., A geometrical theory for spiral waves in excitable media, *SIAM J. Appl. Math.* 46, 1039-1056, 1986.

[47] Keller, E.F. and Segel, L.A., Initiation of slime mold aggregation viewed as an instability, *J. Theor. Biol.* 26, 399-415, 1970.

[48] Kishimoto, K. and Weinberger, H.F., The spatial homogeneity of stable equilibria of some reaction-diffusion systems on convex domains, *J. Diff. Equations* 58, 15-21, 1985.

[49] Kolmogorov, A., Petrovsky, I., and Piskunov, N., Study of the diffusion equation with growth of the quantity of matter, and its application to a biology problem. *Bul. Moskovskovo Gos. Univ.* 17, 1-26, 1937, (in Russian). English translation in *The Dynamics of Curved Fronts* P. Pelcé, Ed., Academic Press, New York, 1988.

[50] Krishnan, J., Iglesias, P.A., and Ma, L., Spatial sensing of chemotactic gradients: a reaction-diffusion approach, preprint (2002).

[51] Kuramoto, Y., *Chemical Oscillations, Waves and Turbulence*, Springer Series in Synergetics, Heidelberg, 1984.

[52] Ladyzenskaja, O.A., Solonnikov, V.A., and Uraltseva, N.N., *Linear and Quasilinear Equations of Parabolic Type*, Transl. Math. Monographs. vol. 23, AMS, Providence, RI, 1968.

[53] Larson, D.A., Transient bounds and time-asymptotic behavior of solutions to nonlinear equations of Fisher type, *SIAM J. Appl. Math.* 34, 93-103, 1978.

[54] Levchenko, A. and Iglesias, P. A., Models of eukaryotic gradient sensing: applications to chemotaxis of amoebae and neutrophils, *Biophysical J.* 82, 50-63, 2002.

[55] N. G. Lloyd, *Degree Theory*, Cambridge University Press, London, New York, 1978.

[56] Matano, H., Asymptotic behaviour and stability of solutions of semilinear diffusion equations, *Publ. RIMS, Kyoto Univ.* 15, 401-454, 1979.

[57] Matano, H. and Mimura, M., Pattern formation in competition-diffusion systems in nonconvex domains, *Publ. RIMS, Kyoto Univ.* 19, 1049-1079, 1983.

[58] Meinhardt, H., Morphogenesis of lines and nets, *Differentiation* 6, 117-123, 1976.

[59] Meinhardt, H., *Models of Biological Pattern Formation*, Academic Press, New York, 1982.

[60] Meinhardt, H., Orientation of chemotactic cells and growth cones: models and mechanisms, *J. Cell Science* 112, 2867-2874, 1999.

[61] Mikhailov, A.S., *Foundations of Synergetics I*, Springer Verlag, Heidelberg, 1994.

[62] Ming, G.-L., Wang, S.T., Henley, J., Yuan, X.B., Song, H.J., Spitzer, N.C., and Poo, M.M., Adaptation in the chemotactic guidance of nerve growth cone, *Nature* 417, 411-418, 2002.

[63] Murray, J.D., *Mathematical Biology*, Springer, Heidelberg, 1993.

[64] Nagai, T., Blow-up of radially symmetric solutions to a chemotaxis system, *Adv. Math. Sci. Appl.*, 1-21, 1995.

[65] Nanjundiah, V., Chemotaxis, signal relaying, and aggregation morphology, *J. Theor. Biol.* 42, 63-105, 1973.

[66] Neu, J.C., Chemical waves and the diffusive coupling of limit cycle oscillators, *SIAM J. Appl. Math.* 36, 509-515, 1979.

[67] Neu, J.C., Coupled chemical oscillators, *SIAM J. Appl. Math.* 37, 307-315, 1979.

[68] Neu, J.C., Large populations of coupled chemical oscillators, *SIAM J. Appl. Math.* 38, 305-316, 1980.

[69] Oelschläger, K., On the derivation of reaction-diffusion equations as limit dynamics of systems of moderately interacting stochastic processes, *Prob. Theor. Rel. Fields* 82, 565-581, 1989.

[70] Oss, C.V., Panfilov, A.V., Hogeweg, P., Siegert, F., and Weijer, C.J., Spatial pattern formation during aggregation of the slime mould Dictyostellium discoideum, *J. Theor. Biol.* 181, 203-213, 1996.

[71] Othmer, H.G., and Hillen, T., The diffusion limit of transport equations II: chemotaxis equations, *SIAM J. Appl. Math.* 62, 1222-1250, 2002.

[72] Pazy, A., *Semigroups of Linear Operators and Applications to PDE*, Springer, Heidelberg, 1983.

[73] Ramón y Cajal, S., Sobre la aparición de las expansiones celulares en la médula embrionaria, *Gaceta Sanitaria de Barcelona* 12, 413-419, 1890.

[74] Ramón y Cajal, S., La retine des vertébrés, *La Cellulle* 9, 119-258, 1893.

[75] Rashewsky, N., An approach to the mathematical biophysics of biological self-regulation and cell polarity, *Bull. Math. Biophys.* 2, 15-25, 1940.

[76] Rinzel, J. and Keller, J.B., Travelling wave solutions of a nerve conduction equation, *Biophysical J.* 13, 1313-1337, 1973.

[77] Rinzel, J. and Terman, D., Propagation phenomena in a bistable reaction-diffusion system, *SIAM J. Appl. Math.* 42, 1111-1137, 1980.

[78] Rothe, F., *Global Solutions of Reaction-Diffusion Systems*, Springer Lecture Notes in Mathematics n° 1072, Heidelberg, 1984.

[79] Schiff, L.I., *Quantum Mechanics*, McGraw-Hill, New York, 1968.

[80] Song, H.-J. and Poo, M.-M., The cell biology of neuronal navigation, *Nature Cell Biol.* 3, E81-E88, 2001.

[81] Stevens, A., The derivation of chemotaxis equations as limit dynamics of moderately interacting stochastic many-particle systems, *SIAM J. Appl. Math.* 61, 183-212, 2000.

[82] Strogatz, S.H., From Kuramoto to Crawford: exploring the onset of synchronization in populations of coupled oscillators, *Physica D* 25, 1-20, 2000.

[83] Tessier-Lavigne, M. and Goodman, C.S., The molecular biology of axon guidance, *Science* 274, 1123-1133, 1996.

[84] Turing, A. M., The chemical basis of morphogenesis, *Phil. Trans. R. Soc. London* 237, 37-72, 1952.

[85] Uchiyama, K., The behaviour of solutions of some nonlinear diffusion equations for large times, *J. Math. Kyoto Univ.* 18, 453-508, 1978.

[86] Velázquez, J.J.L., Stability of some mechanisms of chemotactic aggregation, *SIAM J. Appl. Math.* 62, 1581-1633, 2002.

[87] Velázquez, J.J.L., Point dynamics in a singular limit of the Keller-Segel model. To appear in *SIAM J. Appl. Math.* A preprint can be downloaded at `http://www.mat.ucm.es/deptos/ma`.

[88] Velázquez, J.J.L., Well posedness of a model of point dynamics for a limit of the Keller-Segel system. Submitted for publication 2002. A preprint can be downloaded at `http://www.mat.ucm.es/deptos/ma`.

[89] Weinberger, H.F., *A First Course in Partial Differential Equations*, Dover, New York, 1995.

[90] Whitham, G.B., *Linear and Nonlinear Waves*, Wiley Interscience, New York, 1974.

[91] Winfree, A.T., *The Geometry of Biological Time*, Springer Verlag, Heidelberg, 1980.

[92] Winfree, A.T., *When Time Breaks Down*, Princeton Univ. Press, Princeton, NJ, 1987.

ANALYTIC INDEX